Lawrence Berkeley National Laboratory
Recent Work

Title
ON THE EQUAL MASS SPACING OF THE DECUPLED OP JP = 3/2 BARTONS

Permalink
https://escholarship.org/uc/item/7bp2g6rj

Author
Slansky, Richard Cyril.

Publication Date
1967-03-15

University of California

Ernest O. Lawrence
Radiation Laboratory

ON THE EQUAL MASS SPACING OF THE DECUPLET OF
$J^P = 3/2^+$ BARYONS

DISCLAIMER

UNIVERSITY OF CALIFORNIA

Lawrence Radiation Laboratory
Berkeley, California

ON THE EQUAL MASS SPACING OF THE DECUPLET OF $J^P = 3/2^+$ BARYONS

Richard Cyril Slansky

(Ph. D. Thesis)

March 15, 1967

ON THE EQUAL MASS SPACING OF THE DECUPLET OF $J^P = 3/2^+$ BARYONS

Contents

ON THE EQUAL MASS SPACING OF THE DECUPLET OF $J^P = 3/2^+$ BARYONS

Richard Cyril Slansky

Lawrence Radiation Laboratory
University of California
Berkeley, California

March 16, 1967

ABSTRACT

With the assumption that the unperturbed amplitude is known in the ND^{-1} representation, equations are derived for calculating the perturbed amplitude as a function of the variations of the left-hand singularities and the unitarity cuts. Exact formulas for mass and coupling-constant shifts of bound states of the unperturbed amplitude are given, and the equations are then iterated to yield a perturbation theory.

The response of the decuplet masses to octet perturbations of the meson and baryon masses and couplings is studied in an ND^{-1} model of baryon-meson scattering, and it is found that the equal mass spacing of the decuplet is satisfied, even for large values of the symmetry breaking. The numerical inaccuracy of several forms of perturbation theory indicates that the physical baryon masses represent a large symmetry breaking in the calculation of the decuplet; so large that first- and second-order perturbation theories do not explain the equal mass spacing of the decuplet, although experiment and the exact solution to the model do give equal spacing. The rapid breakdown of

the octet sum rules for the S-matrix elements also suggests that the SU(3) violations are large, and that the octet output is special to the masses.

PART A

THE MASS SPACING OF THE DECUPLET

I. INTRODUCTION

The existence and mass of the Ω^- particle were predicted from the unitary symmetry model.[1] The $N_{3/2}^*(1236)$ and $Y_1^*(1385)$ particles were already established experimentally when evidence for the $\Xi_{1/2}^*(1530)$ was presented.[2] Gell-Mann immediately conjectured that these nine particles belonged to a decuplet representation of SU(3), and that a tenth particle with hypercharge, $Y = -2$, and isospin, $I = 0$, should complete this supermultiplet. With some simple assumptions about the breaking of the SU(3) symmetry, Gell-Mann also predicted the mass of this baryon, which he christened the Ω^-.[1] Over a year later, the Ω^- was observed at the predicted mass.[3] This remarkable discovery corroborated the existence of a decuplet of $J^P = 3/2^+$ baryons: $N_{3/2}^*(1236)$ with $I = 3/2$ and $Y = +1$ (which we refer to as the N^*); $Y_1^*(1385)$ with $I = 1$ and $Y = 0$ (referred to as the Y^*); the $\Xi_{1/2}^*(1530)$ with $I = \frac{1}{2}$ and $Y = -1$ (referred to as the Ξ^*); and the Ω^- with a mass of 1674 MeV, $I = 0$, and $Y = -2$.

The mass splitting of the decuplet is reproduced within 2% by the formula,

$$m_Y = a + b Y , \qquad (1.1)$$

where $a = 1385$ MeV, $b = 147$ MeV, and m_Y is the mass of the particle with hypercharge, Y. The mass splitting is just proportional to the hypercharge, a result which follows from the simple (broken) symmetry model. Although the equal mass spacing of the decuplet of baryon resonances predicted by $SU(3)$ has been confirmed experimentally, the high accuracy of Eq. (1.1) has not been satisfactorily explained from more fundamental theoretical considerations.

The usual derivation of Eq. (1.1) is basically group theoretical, with a and b to be determined from experiment. We assume the existence of a mass operator which transforms in $SU(3)$ space as a singlet plus the $I = 0$, $Y = 0$ member of an octet. (Another member of an octet would violate I or Y conservation.) The mass of the particle is just the expectation value of the mass operator. A short calculation then yields equal mass spacing for the decuplet.

As it stands, this simple theory is far from being a complete dynamical theory for two (related) reasons: it does not account for the origin of the mass operator and it gives no reason for neglecting the $I = 0$, $Y = 0$ members of the $\underline{27}$ and $\underline{64}$ representations which also occur in $\underline{\widetilde{10}} \otimes \underline{\widetilde{10}}$. In simple field-theoretic models, the Hamiltonian, which is expanded into a singlet plus as octet tensor, is used to construct the mass operator. In first order, the mass operator (self energy operator) also transforms just as a singlet plus an octet. In this case, Eq. (1.1) has theoretical significance only for small values of the symmetry breaking. The dominance of octet

symmetry breaking[4] can be understood from dynamical theories, at least for small symmetry breaking. However, only the experimental masses suggest octet dominance (or $\underline{27}$ and $\underline{64}$ suppression) in the simple group theoretical model. It is clear that any investigation of the theoretical basis of the equal spacing rule must incorporate some dynamics into the group theory (or vice versa).

We use a simple dynamical model of the decuplet to investigate its equal mass spacing. The model reproduces many features of the analytic S matrix. In S-matrix dynamics,[5] at least some particles are generated by the channels with which they communicate (i.e., the channels that have the same quantum numbers as the particle itself) and by the interaction mechanism. Unitarity and analyticity may then imply other singularities that are not already apparent from the input. Poles which appear in the analytically-continued amplitude are identified as composite particles.

Several features of SU(3) guide the selection of a dynamical model. Most basic to the model is the choice of scattering channels and the interaction mechanism; the "Eightford Way" classification scheme[2] is useful in making a "reasonable" choice. The simplest set of channels suggested by SU(3) which contain the same quantum numbers as the decuplet is the set of two-body channels composed of one baryon from the $J^P = \frac{1}{2}^+$ baryon octet and one meson from the $J^P = 0^-$ pseudoscalar-meson octet. With a single-baryon-exchange interaction, the decuplet can be a bound state of these channels.[6]

So the obvious requirement that the decuplet must exist is satisfied
in this model. Deviations from pure SU(3) symmetry are easily
included. The masses of the baryon octet and pseudoscalar-meson
octet appear in the dynamical equations. Consequently, octet symmetry
breaking of the baryon (and meson) masses is incorporated by requiring
that the masses satisfy the Gell-Mann-Okubo sum rule. In the single-
baryon-exchange model, the baryon-meson coupling constants are
conveniently found from the unitary symmetry model. If the dominant
channels are the two body baryon-meson channels, then we use the two-
body-multichannel S matrix.

There is one pleasant feature of our investigation which allows
some radical approximations. We are not interested here in calculating
meson-baryon scattering amplitudes for arbitrary energy. We only need
the location of the bound-state pole. Moreover, we do not attempt to
calculate the exact physical masses of the decuplet.. Our purpose is
simply to investigate the mass <u>spacing</u> of the decuplet. Thus,
approximations which do not destroy the features of the mass spacing
are certainly valid for our purposes.

Since the decuplet particles are all p-wave states, we consider
the partial wave amplitude where two-body unitarity is particularly
simple. Direct channel unitarity is an important ingredient of the
dynamics, so we guarantee it by using the N/D equations for the
partial-wave amplitude. Although it is difficult to treat cross-channel
unitarity in a satisfying manner, the mass <u>spacing</u> of the decuplet is

rather insensitive to large changes of the left singularities.
Therefore, as we discuss in Section II, it is sufficient to approximate
the left singularities by a pole.

One last simplification concerns the spin kinematics. Since
the total angular momentum is a half odd integer for meson-baryon
scattering, it is appropriate to work in the $w = \sqrt{s}$ plane. Then
the once subtracted dispersion integral in the D function is
logarithmically divergent. However, the qualitative features of the
mass spacing are not changed if we consider scalar baryons, and look
for the spin one decuplet in the $\ell = 1$ scattering amplitude. On
comparision with similar models using fermion kinematics, we find that
the only change resulting from the scalar kinematics is that the
decuplet masses satisfy a mass-<u>squared</u> equal spacing rule for large
symmetry breaking.

In summary, our investigation of the decuplet mass spacing is
based on a model of baryon-meson scattering by single-baryon exchange.
Unitarity in the direct channel is guaranteed by the ND^{-1} equations,
and the model is easily solved if the left singularities are approximated
by a pole. The computation is greatly facilitated by using scalar
kinematics. The details of the model and justifications of our
approximations are found in Section II. Some of the lengthy calculations
necessary for the solution of the model are included in three
appendices. The Yukawa couplings, including octet symmetry breaking,
are calculated from $SU(3)$ in Appendix I. The isospin crossing matrices

are found in Appendix II, and several dispersion integrals are integrated in Appendix III.

In Section III, we begin the investigation of the mass splitting of the decuplet. If the external baryon and meson masses and couplings are set at their SU(3) degenerate values, then all four decuplet isomultiplets (which we refer to as particles) will have the same mass. While requiring that the octet sum rules remain satisfied, we "turn on" the octet perturbations of the external baryon and meson masses (or couplings). As the symmetry breaking increases, we observe the induced mass splitting of the output decuplet. (This is done by solving $\det[D(s)] = 0$.) The mass splitting of the decuplet increases, and equal spacing is satisfied for values of the symmetry breaking comparable with the physical symmetry breaking. However, the mass splitting deviates markedly from being a linear function of the input symmetry breaking.

The most noteworthy feature of these calculations is the stability of the equal spacing. Octet symmetry breaking input in the baryon and meson masses and couplings produces octet symmetry breaking output in the decuplet masses over large ranges of the symmetry breaking parameters. Equal spacing is certainly expected for small values of the symmetry breaking, as is easily proven. However, as nonlinear effects become important, it is not obvious why the equal spacing should continue to be so well satisfied.

We further investigate the nonlinearities with several forms of perturbation theory. In Section IV, we expand in the mass perturba-

tions[7] of the external baryons and mesons, and compare the mass expansions with the results of Section III. The first-order mass expansion preserves equal spacing, as expected. However, after the mass splitting of the baryons has been turned on to above half the physical amount, the first-order results become bad approximations to the exact results of the model. Although the second-order mass expansion appears to satisfy equal spacing, the accuracy of the second-order calculation breaks down rather soon after the first-order theory. When the masses of the baryons and mesons approach their physical values, both the first- and second-order approximations are in bad agreement with the exact result.

The results of Section IV indicate that any first-order perturbation theory will yield inaccurate results for the physical mass splittings of the baryons and mesons. However, the Dashen-Frautschi first-order perturbation theory[8] has been applied to the octet enhancement calculation for the decuplet, and so it is useful to gain some quantitative feeling for its accuracy. In Section V, we compare the numerical results of the first-order Dashen-Frautschi theory to the solutions of the model found in Section III.

In Sections II through V, we emphasize that the equal mass spacing of the decuplet appears to be more than a first-order result; nonlinear effects are appreciable for physical mass values of the external baryons and mesons. However, it is possible that the mass splitting of the decuplet is a linear effect if the baryon-meson

channels are much more massive than the $J^P = \frac{1}{2}^+$ baryon-pseudoscalar-meson channels. Since heavier octets of baryons should contribute to the binding of the decuplet, it is reasonable to examine whether the nonlinear effects are reduced by replacing the external baryons by more massive particles. This idea is examined in Section VI, and we find that although the nonlinear effects are reduced, they are still appreciable for 4 BeV external baryons. However, for 9 BeV external baryons, the Dashen-Frautschi formula is reasonably accurate when the decuplet mass spacing is at its physical value of 150 MeV [or about 0.43 $(BeV)^2$].

In the simple field-theoretic model, where the Hamiltonian is expanded into a singlet plus an octet tensor, the amplitude is also a singlet plus an octet to first order. In the dispersion theoretic calculations, the mass breaking satisfies the octet sum rule for large symmetry breaking. In Section VII, we test whether the amplitude satisfies octet sum rules for large symmetry breaking. We find that the sum rules are satisfied only for small perturbations that are less than half the physical symmetry breaking of the baryon and meson masses.

In Part B of the thesis we propose exact equations for mass and coupling shifts in dispersion theory. With the assumption that the unperturbed amplitude is known in the ND^{-1} representation, equations are derived for calculating the perturbed amplitude as a function of the variations of the left-hand singularities and the unitarity cuts. Exact formulas for the mass and coupling-constant shifts of bound states of the unperturbed amplitude are given, and the equations are then iterated to yield a perturbation theory.

II.   A MODEL FOR THE MASS SPACING OF THE DECUPLET

The model for calculating the mass spacing of the decuplet is described in this section. If the $J^P = \frac{3}{2}^+$ baryons are composite systems, then the simplest set of channels that communicates with the decuplet is the set of two-body baryon-meson channels.[6] Consider all the two-body baryon-meson channels having a particular value of I and Y. Then the N^* communicates with the $N\pi$ and ΣK channels; the Y_1^* with the $N\bar{K}$, $\Sigma\pi$, $\Lambda\pi$, ΞK, and $\Sigma\eta$ channels; the Ξ^* with the $\Xi\pi$, $\Lambda\bar{K}$, $\Sigma\bar{K}$, and $\Xi\eta$ channels; and the Ω^- with the $\Xi\bar{K}$ channel. Although the decuplet-meson channels, three-body channels, and other channels all contribute to the mass of the decuplet they have not been included. We do not expect this approximation to affect the mass spacing results of the model in any qualitative way.

Another basic assumption in our dynamics is the importance of the single-baryon exchange diagram for binding the decuplet. Many other diagrams will contribute to the exact mass of the decuplet, however, again the mass spacing is not qualitatively affected by the neglect of more complicated forces.

The most important property of the S matrix for our study is unitarity in the direct channel, so we unitarize the single-baryon exchange diagram with the ND^{-1} method.

The two-body multichannel S matrix is

$$S_{fi} = \delta_{fi} + i(2\pi)^4 (16\,\omega_f E_f \omega_i E_i)^{-\frac{1}{2}} \delta^4(p_f + q_f - p_i - q_i) T_{fi}(s,t) \tag{2.1}$$

with the integral relation implied by Eq. (2.7), Eq. (2.8) is a
set of coupled integral equations for $D_{ij}(s)$.

The model in which $f(s)$ is just the discontinuity across the
Born cuts was first considered by Martin and Wali[6] (with fermion
kinematics). They solved Eq. (2.8) in the first-order determinental
approximation, but without simplifications of the Born cuts. Later,
Wali and Warnock[9] showed that the meson and baryon mass differences
have their strongest effects in the phase space factor, $\rho(s)$, and
not in the Born exchange term. They were able to duplicate the results
of Martin and Wali by fixing the masses of the exchange baryons at a
degenerate value, and thus greatly reduce the computational labor.

We take seriously the suggestion that the qualitatively
important features of the decuplet mass splitting are due to unitarity
in the direct channel, and not to the fine details of the left
singularities. Thus it is possible that a pole approximation to the
left cuts will lead to essentially the same mass spacing as the exact
solution to the N/D equations with the full Born cuts. In fact,
we find that the spacing is very insensitive to the location of the pole.

If the left cut is approximated by a pole, then the solution of
the dispersion relation for $N(s)$ is

$$N(s) \; = \; N_0 \, (s - t)^{-1} \, D(t), \qquad\qquad (2.9)$$

where N_0 is a matrix of products of coupling constants and t is

the position of the pole. We set the subtraction point in $D(s)$ equal to the pole location in $N(s)$. The exact solution for $D(s)$ is found by substituting Eq. (2.9) into Eq. (2.8),

$$D_{ij}(s) = \delta_{ij} - \frac{(s - t)}{(8\pi)^2}$$

$$\int_{(M_i + \mu_i)^2}^{\infty} dx \; \frac{[x^2 - 2(M_i^2 + \mu_i^2) s + (M_i^2 - \mu_i^2)^2]^{3/2}}{x^2 (x - t)^2 (x - s - i\epsilon)} \; (N_0)_{ij} \; . \tag{2.10}$$

After the matrix elements of N_0 are computed and the integrals evaluated, we search for the bound states. This part of the calculation is usually carried out by solving

$$\det[D(s_R + is_I)] = 0, \tag{2.11}$$

where s_R is the mass squared of the resonance. Wali and Warnock[9] have shown that the solution to Eq. (2.11)

$$\det[\text{Re } D(s_R)] = 0 \tag{2.12}$$

is a good approximation to the solution of Eq. (2.11), since the widths of the resonances are small compared to their masses. Moreover, Eq. (2.12) is just the condition for a pole in the K matrix. By assuming that the particle mass is the location of the pole in the K matrix, we avoid complex arithmetic on the computer while retaining

a good approximation to the solution of Eq. (2.11). The decuplet

masses in the following calculations are solution to Eq. (2.12).

The model is completed except for finding explicit expressions

for N_0. We merely outline the calculation here; the details are

ennumerated in the appendices. To find N_0, we need the (broken)

SU(3) baryon-meson couplings[10] and the isospin crossing matrices[11]

(in order to compute the contribution of each exchange to the isospin

state being considered).

The coupling constants are calculated on the assumption that

the interaction Hamiltonian for the BBP vertex is given by

$$H_{int} = g_{bdg}^{ace} \bar{B}_a^b B_c^d P_e^g , \qquad (2.13)$$

where $\bar{B}_a^b$ are the components of the octet of antibaryons, B is the

octet tensor of baryons, and P is the octet tensor of pseudoscalar

mesons. The decomposition of $\underset{\sim}{8} \otimes \underset{\sim}{8} \otimes \underset{\sim}{8}$ contains two singlet

representations and eight octets. If the SU(3) symmetry breaking

force is dominated by the I = 0, Y = 0 member of an octet, and if

H_{int} is hermitian, then two pure symmetry and five symmetry breaking

parameters determine the $\bar{B}$BP couplings. After a lengthy but

straightforward calculation (see Appendix I for details), we find

that the meson-baryon couplings in units of an overall coupling

constant g are

$$g_{NN\pi} = 1 + (2/3)\,\epsilon_1$$

$$g_{\Sigma\Lambda\pi} = (2/\sqrt{3})\,(1 - f - \epsilon_5)$$

$$g_{\Sigma\Sigma\pi} = 2f + (2/3)\,\epsilon_1 - \epsilon_2 - (2/3)\,\epsilon_3$$

$$g_{\Xi\Xi\pi} = -\left(1 - 2f + (2/3)\,\epsilon_3\right)$$

$$g_{N\Lambda K} = -\sqrt{3}\,(1 + 2f + \epsilon_2 + \epsilon_3 + 2\,\epsilon_s)$$

$$g_{N\Sigma K} = 1 - 2f - (1/3)\,\epsilon_3$$

$$g_{\Lambda\Xi K} = -\sqrt{3}\,(1 - 4f + \epsilon_1 - \epsilon_2 + 2\epsilon_5)$$

$$g_{\Xi\Sigma K} = -1 + (1/3)\,\epsilon_1$$

$$g_{NN\eta} = -\sqrt{3}\,(1 - 4f - \epsilon_2 - 2\epsilon_3 + 2\epsilon_4)$$

$$g_{\Lambda\Lambda\eta} = -(2/\sqrt{3})\,(1 - f + \epsilon_4 + 2\epsilon_5)$$

$$g_{\Sigma\Sigma\eta} = (2/\sqrt{3})\,(1 - f - \epsilon_4)$$

$$g_{\Xi\Xi\eta} = -(1/\sqrt{3})\,(1 + 2f - 2\epsilon_1 + \epsilon_2 + 2\epsilon_4)\,. \tag{2.12}$$

The F to D ratio is related to f by

$$f = g_F (g_F + g_D)^{-1},$$

(2.13)

and $\epsilon_1, \cdots, \epsilon_5$ are the octet symmetry breaking parameters.

The calculation of N_0 is easily completed once the isospin crossing matrices are known. Since it is somewhat tricky to get all the phases[11] correct, we have included a detailed derivation of the crossing matrices in Appendix II. The matrix, N_0 , for each of the four sets of decuplet quantum numbers is displayed in Table 1.

In Appendix III, the integrals in Eq. (2.10) are evaluated analytically in order to expedite numerical calculations.

The arbitrary parameters of the model are: (i) the exchange pole position, the overall coupling constant (the $\overline{N}N\pi$ coupling with no symmetry breaking), and the F/D ratio, f; (ii) the external baryon and meson masses; and (iii) the parameters ϵ_1 through ϵ_5 that characterize the octet symmetry breaking of the baryon-meson coupling constants. We now solve Eq. (2.12) for many values of these parameters. Variations of t, g, and f are done below; the results of (ii) and (iii) comprise Section III. The numerical solutions of Eq. (2.12) were found by the Physics Department's IBM 1620 computer in Birge Hall at the University of California, Berkeley.

The object of the following three calculations is to show that the decuplet mass spacing is not sensitive to the precise numerical values of g, t, and f. In all three discussions, the baryon-meson

couplings are set at the SU(3) degenerate values. (The NNπ

coupling constant is equal to g for zero octet symmetry breaking

of the couplings.)

In Fig. 1, the decuplet masses are shown as a function of

g. We set $t = -1$ $(BeV)^2$, $f = 0.33$, and the baryon and meson masses

equal to their physical values. The most notable feature of Fig. 1

is that for fixed $g > 16$, the mass spacings $(m_{Y^*}^2 - m_{N^*}^2, m_{\Xi^*}^2 - m_{Y^*}^2,$

and $m_{\Omega^-}^2 - m_{\Xi^*}^2)$ are always within 3% of one another. For $g < 16$,

the input forces are barely strong enough to bind the decuplet, and

the equal spacing begins to break down appreciably. However, for

$g > 16$, the mass spacing is very stable, and, in fact, the mass spacing

itself changes only very slowly as a function of g . So the spacing

of the decuplet is quite independent of g , at least for (approximate)

octet symmetry breaking input, i.e., the physical baryon and meson

masses.

It is possible that octet symmetry breaking is a special case

and the spacing properties are not stable unless the baryon and meson

masses satisfy the Gell-Mann-Okubo sum rule. If the symmetry breaking

of the baryon masses is not octet, then the decuplet masses are not

equally spaced. However, the curves representing the decuplet masses

as a function of g are approximately parallel to those shown in Fig. 1.

As an example of baryons that are very far from satisfying the Gell-

Mann-Okubo sum rule: $m_N = m_\Xi = 1500$ MeV; $m_\Lambda = m_\Sigma = 900$ MeV;

$m_\pi = m_K = m_\eta = 137$ MeV ; $\frac{1}{2}(m_N^2 + m_\Xi^2) = 2.25$ $(BeV)^2$; and

$\frac{3}{4} m_\Lambda^2 + \frac{1}{4} m_\Sigma^2 = 0.81 \ (\text{BeV})^2$. (Because of the scalar kinematics, we use mass-squared sum rules. By "equal mass spacing", we always mean that the mass-squared spacings are equal.) As in Fig. 1, the spacing is very stable for $g > 16$: the N^* is a few hundreths of a $(\text{BeV})^2$ heavier than the Y_1^*; and the spacing between the Y_1^* is about one seventh of the spacing between the Ξ^* and the Ω^-. We conclude that the mass spacing of the decuplet is quite independent of g; we set $g = 19$.

Figure 2 shows the decuplet masses as a function of t (t is the subtraction point and exchange pole position). The baryon and meson masses are equal to their physical values; $g = 19$; and $f = 0.33$. As t is varied from $-0.1 \ (\text{BeV})^2$ to $-5 \ (\text{BeV})^2$, the decuplet masses all slowly decrease, which is a typical result of N/D models in the pole approximation. The mass spacings for each t are equal within 2%. Also, the mass spacing itself changes very little over the range; at $t = -0.1 \ (\text{BeV})^2$ the mass spacing is $0.545 \ (\text{BeV})^2$; and at $t = -5 \ (\text{BeV})^2$ the spacing is $0.500 \ (\text{BeV})^2$. (However, compare with Ref. 9. We repeat that the pole is meant to approximate the entire set of left singularities and not just the Born cuts.)

The F/D ratio is varied in Fig. 3. For fixed f in the range $0 < f < 0.45$, the mass spacings are equal within 2%. Outside this range, the equal spacing slowly breaks down as the decuplet becomes unbound. According to the model of Martin and Wali,[6] the decuplet exists only for $-0.28 < f < 0.78$; the same is approximately

true in our model. In the range $0 < f < 0.45$, the spacing is insensitive to f .

We see from Figs. 1, 2, and 3, that the spacings of the decuplet are quite insensitive to variations of g, t, and f over large ranges of these parameters. Also, the actual value of the mass spacing is not very dependent on g, t, or f . Thus, for physical baryon and meson masses and SU(3) symmetric couplings, the value of the mass spacing is not really a free parameter. If t, g, and f are arranged so that the mass of the N^* is 1236 MeV, then the mass of the Ω^- is about 1785 MeV. It is impossible to decrease the Ω^- mass the necessary 100 MeV with any reasonable value of f, t, and g in order to fit both the N^* and Ω^- masses for physical baryon and meson masses and SU(3) symmetric couplings.

We conclude that the mass spacing of the decuplet is insensitive to g, t, and f. However, the mass spacing _is_ sensitive to the symmetry breaking of the baryon and meson masses and couplings, as is shown in the next section. We let $g = 19$, $t = -1 \ (\text{BeV})^2$, and $f = 0.33$.

TABLE 1: The Born Matrices, N_0. (See Eq. (2.9).) The rows and columns of N_0 correspond to the initial and final meson-baryon channels. The phase conventions are those of de Swart.[12] See Appendix II for a derivation and discussion of the isospin crossing matrices necessary in finding N_0.

$I = \frac{3}{2}$, $Y = 1$	$N\pi$	ΣK
$N\pi$	$2g_{NN\pi}^2$	$g_{N\Lambda\pi}\, g_{\Sigma\Lambda\pi} - g_{N\Sigma K}\, g_{\Sigma\Sigma\pi}$
ΣK	$g_{N\Lambda K}\, g_{\Sigma\Lambda\pi} - g_{N\Sigma K}\, g_{\Sigma\Sigma\pi}$	$2g_{\Xi\Sigma K}^2$

$I = 0$, $Y = -2$	$\Xi \bar{K}$
$\Xi \bar{K}$	$3g_{\Xi\Sigma K}^2 - g_{\Xi\Lambda K}^2$

(Table I continued)

Table I continued

$I=1,\ Y=0$	$N\ \bar{K}$	$\Sigma\ \pi$	$\Lambda\ \pi$	$\Xi\ K$	$\Sigma\ \eta$
$N\ \bar{K}$	0	$-2g_{NN\pi}g_{N\Sigma K}$	$-\sqrt{2}g_{NN\pi}g_{N\Lambda K}$	$g_{N\Lambda K}g_{\Xi\Lambda K}$ $+\ g_{N\Sigma K}g_{\Xi\Sigma K}$	$-\sqrt{2}\ g_{NN\eta}\ g_{N\Sigma K}$
$\Sigma\ \pi$	$-2g_{NN\pi}g_{N\Sigma K}$	$g_{\Sigma\Sigma\pi}^{2}-g_{\Sigma\Lambda\pi}^{2}$	$-\sqrt{2}g_{\Sigma\Sigma\pi}g_{\Sigma\Lambda\pi}$	$2g_{\Xi\Sigma K}\ g_{\Xi\Xi\pi}$	$\sqrt{2}\ g_{\Sigma\Sigma\eta}\ g_{\Sigma\Sigma\pi}$
$\Lambda\ \pi$	$-\sqrt{2}g_{NN\pi}g_{N\Lambda K}$	$-\sqrt{2}g_{\Sigma\Sigma\pi}g_{\Sigma\Lambda\pi}$	$g_{\Sigma\Lambda\pi}^{2}$	$\sqrt{2}\ g_{\Xi\Lambda K}g_{\Xi\Xi\pi}$	$g_{\Lambda\Lambda\eta}\ g_{\Sigma\Lambda\pi}$
$\Xi\ K$	$g_{N\Lambda K}g_{\Xi\Lambda K}$ $+\ g_{N\Sigma K}g_{\Xi\Sigma K}$	$2g_{\Xi\Sigma K}\ g_{\Xi\Xi\pi}$	$\sqrt{2}g_{\Xi\Lambda K}g_{\Xi\Xi\pi}$	0	$\sqrt{2}\ g_{\Xi\Xi\eta}\ g_{\Xi\Sigma K}$
$\Sigma\ \eta$	$-\sqrt{2}g_{NN\eta}g_{N\Sigma K}$	$\sqrt{2}\ g_{\Sigma\Sigma\eta}g_{\Sigma\Sigma\pi}$	$g_{\Lambda\Lambda\eta}\ g_{\Sigma\Lambda\pi}$	$\sqrt{2}\ g_{\Xi\Xi\eta}\ g_{\Xi\Sigma K}$	$g_{\Sigma\Sigma\eta}^{2}$

Table I continued

$I = \frac{1}{2}$, $Y = -1$	$\Xi\,\pi$	$\Lambda\,\bar{K}$	$\Sigma\,\bar{K}$	$\Xi\,\eta$
$\Xi\,\pi$	$-g_{\Xi\Xi\pi}^2$	$\sqrt{3}\,g_{\Xi\Sigma K}g_{\Sigma\Lambda\pi}$	$-2g_{\Xi\Sigma K}g_{\Sigma\Sigma\pi} - g_{\Xi\Lambda K}g_{\Sigma\Lambda\pi}$	$\sqrt{3}\,g_{N\Lambda K}\,g_{\Xi\Xi\pi}$
$\Lambda\,\bar{K}$	$\sqrt{3}\,g_{\Xi\Sigma K}g_{\Sigma\Lambda\pi}$	$g_{N\Lambda K}^2$	$\sqrt{3}\,g_{N\Lambda K}g_{N\Sigma K}$	$g_{\Lambda\Lambda\eta}\,g_{\Xi\Lambda K}$
$\Sigma\,\bar{K}$	$-2g_{\Xi\Sigma K}g_{\Sigma\Sigma\pi} - g_{\Xi\Lambda K}g_{\Sigma\Lambda\pi}$	$\sqrt{3}\,g_{N\Lambda K}g_{N\Sigma K}$	$-g_{N\Sigma K}^2$	$-\sqrt{3}\,g_{\Sigma\Sigma\eta}g_{\Xi\Sigma K}$
$\Xi\,\eta$	$3\,g_{N\Lambda K}\,g_{\Xi\Xi\eta}$	$g_{\Lambda\Lambda\eta}g_{\Xi\Lambda K}$	$-\sqrt{3}\,g_{\Sigma\Sigma\eta}g_{\Xi\Sigma K}$	$g_{\Xi\Xi\eta}^2$

FIGURE CAPTIONS

Fig. 1.   Decuplet Masses as Function of g ,   Octet Symmetry Breaking.

Baryon and meson masses are equal to the physical values,

baryon-meson couplings are equal to the SU(3) symmetric

values, f = 0.33, and t = -1 $(BeV)^2$.

Fig. 2.   Decuplet Masses as Function of t .

Baryon and meson masses are equal to the physical values,

baryon-meson couplings are equal to the SU(3) symmetric

values, f = 0.33, and g = 19.

Fig. 3.   Decuplet Masses as Function of f .

Baryon and meson masses are equal to the physical values,

baryon-meson couplings are equal to the SU(3) symmetric

values, g = 19, and t = -1 $(BeV)^2$.

Fig. 1
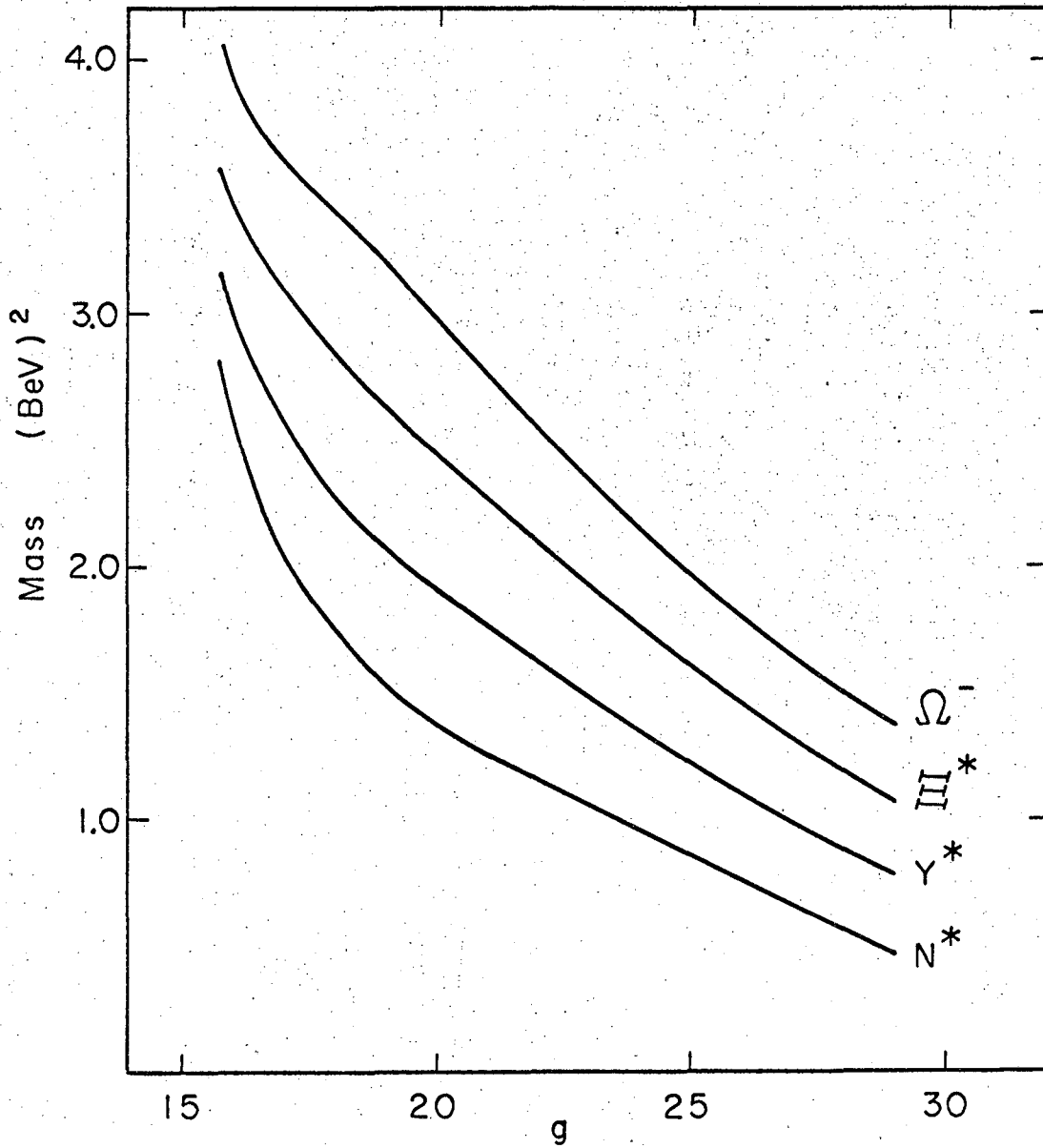
XBL 673 - 2337

Fig. 2
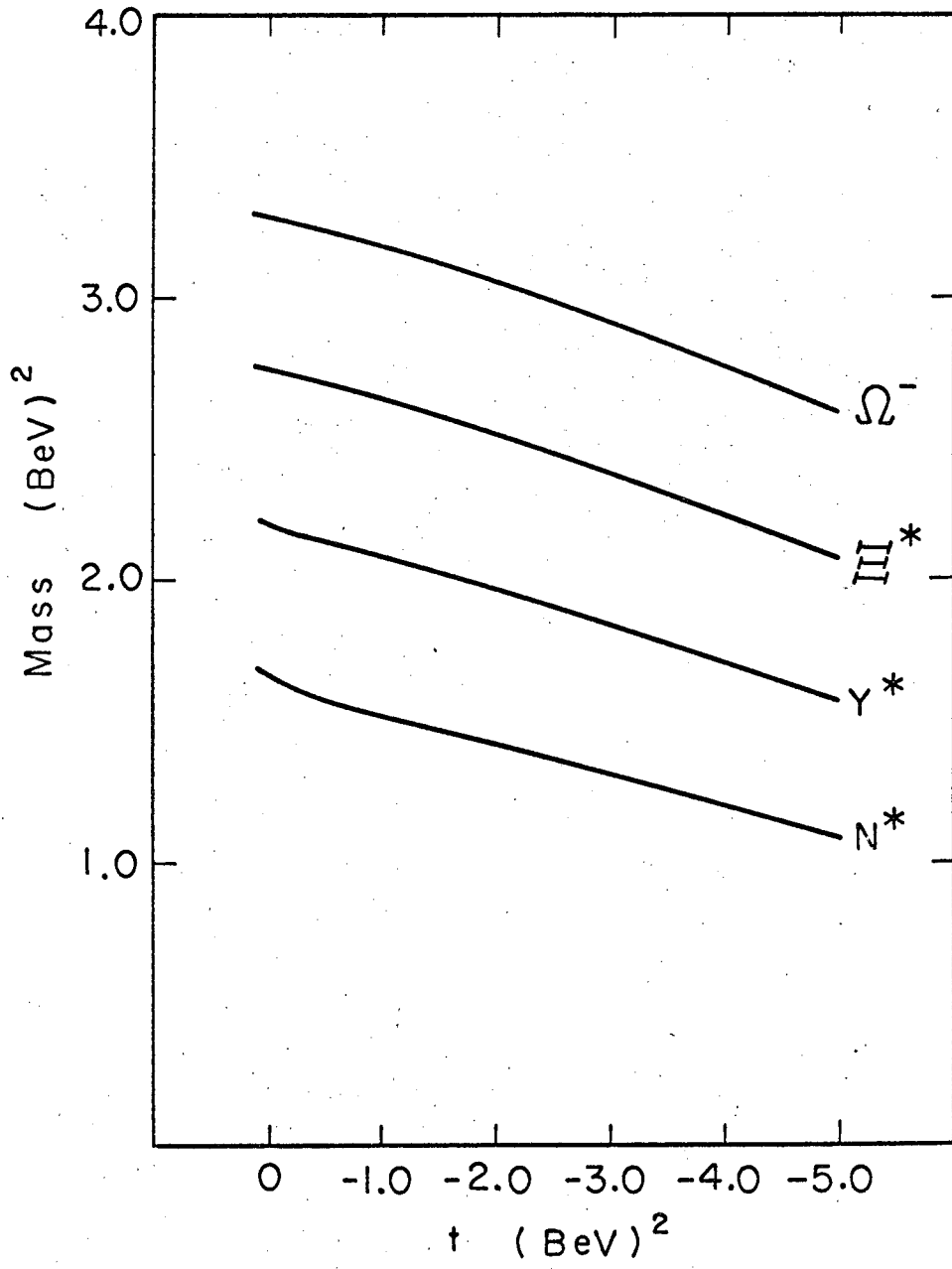
XBL673-2338

Fig. 3
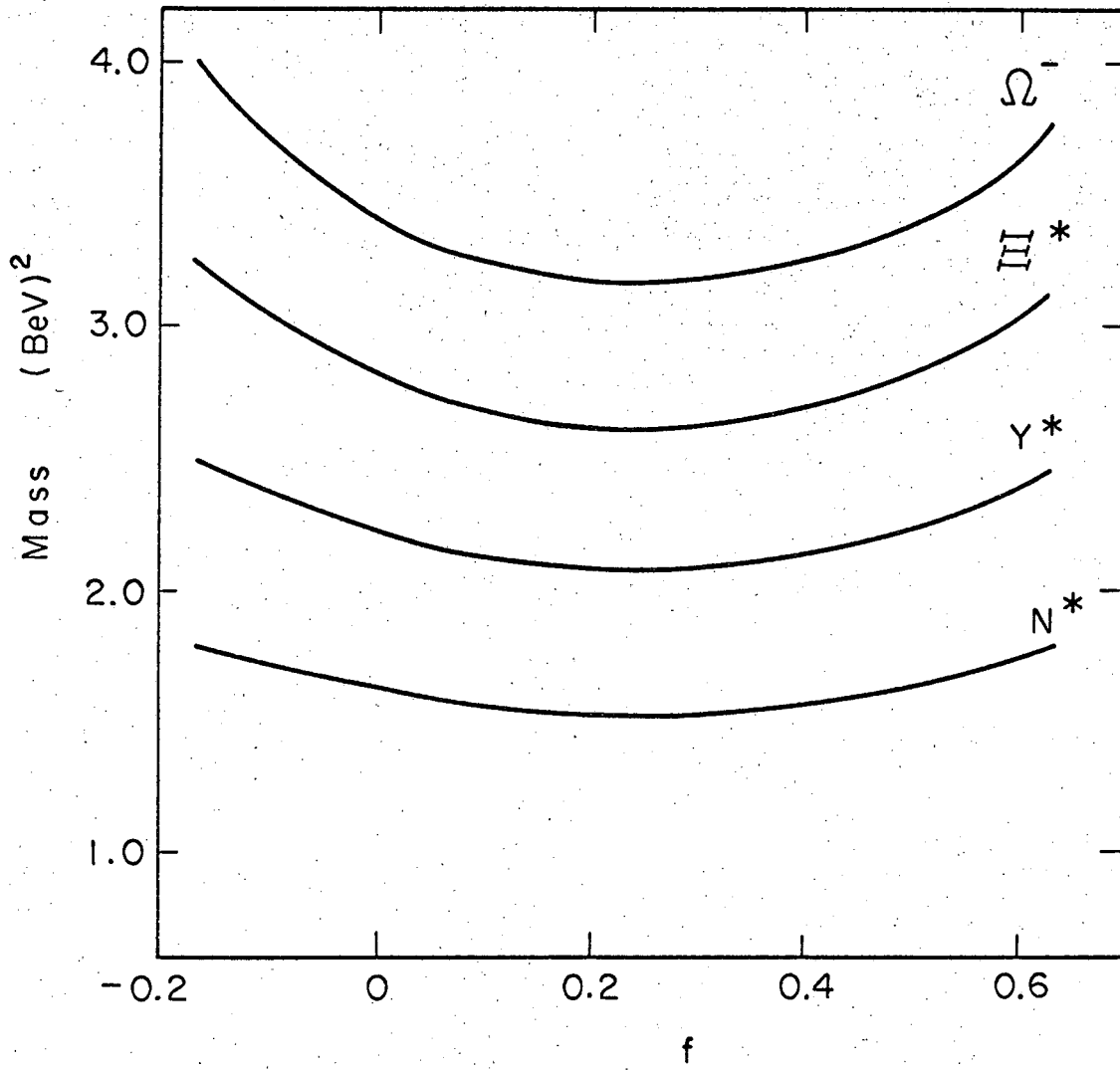
XBL 673-2339

III.   OCTET SYMMETRY BREAKING AND EQUAL MASS SPACING

Section II concluded by showing that the mass spacing of the decuplet is not sensitive to the values of the overall coupling constant, the F/D ratio, or the subtraction point (baryon exchange pole). We select t, g, and f so that for physical baryon and meson masses and $SU(3)$ symmetric couplings, the mass of the N^* is 1236 MeV. However, we cannot fit both the Ω^- and N^* masses by varying g, t, and f, because of the insensitivity of the spacing on these parameters. We set $f = 0.33$, which is near its experimental value, and let $t = -1.$ $(BeV)^2$. Then, $g = 19.$

We now vary the baryon and meson masses and couplings in such a way that the octet symmetry breaking sum rules are always satisfied. The baryon and meson masses (mass-squared) are parameterized to satisfy the Gell-Mann-Okubo sum rule. In units of $(BeV)^2$, they are

$$M_\Sigma^2 = (1.193)^2 \, \delta_1 \, ,$$

$$M_N^2 = M_\Sigma^2 - 0.540 \, \delta_2 \, ,$$

$$M_\Xi^2 = M_\Sigma^2 + 0.316 \, \delta_3 \, ,$$

$$M_\Lambda^2 = M_\Sigma^2 + 0.211 \, \delta_3 - 0.360 \, \delta_2 \, ,$$

$$m_\pi^2 = (0.137)^2 \, \delta_4 \, , \qquad \text{(Equation 3.1 continued)}$$

$$m_K^2 = m_\pi^2 + .266 \; \delta_5 \; ,$$

$$m_\eta^2 = m_\pi^2 + 0.301 \; \delta_5 \; . \qquad\qquad (3.1)$$

The mass <u>squared</u> is <u>linear</u> in the symmetry breaking parameters because of the scalar kinematics. We arrange δ_1 through δ_5 so that for $\delta_1 = \delta_2 = \cdots = \delta_5 = 1$, the baryon and meson masses are close to their physical values: for $\delta_1 = \cdots = \delta_5 = 1$, $m_N = 940$ MeV; $m_\Lambda = 1128$ MeV; $m_\Sigma = 1193$ MeV; $m_\Xi = 1318$ MeV; $m_\pi = 137$ MeV; $m_K = 495$ MeV; and $m_\eta = 565$ MeV. The baryon-meson couplings, including the octet symmetry breaking terms, are listed in Eq. (2.12); the octet symmetry breaking is parameterized by ϵ_1 through ϵ_5. The SU(3) symmetric couplings are recovered by setting $\epsilon_1 = \epsilon_2 = \cdots = 0$.

In most of the following calculations, the equal mass spacing of the decuplet is satisfied within several percent. Therefore it is difficult to measure the deviation from equal spacing from a plot of the decuplet masses. To remedy this inconvenience, we have listed in Table 2 the maximum deviation of the spacings from the average spacing. We define

$$\sigma_1 = m_{Y^*}^2 - m_{N^*}^2$$

$$\sigma_2 = m_{\Xi^*}^2 - m_{Y^*}^2 \; .$$

$$\sigma_3 = m_{\Omega^-}^2 - m_{\Xi^*}^2$$

$$\sigma_A = (\sigma_1 + \sigma_2 + \sigma_3) / 3 . \qquad (3.2a)$$

Then the maximum deviation from the average spacing is

$$d_M = |\max[(\sigma_i - \sigma_A)/\sigma_A]| . \qquad (3.2b)$$

In Fig. 4, the decuplet masses are plotted as a function of the mass breaking parameter, $\delta = \delta_2 = \delta_3 = \delta_5$. The Σ mass and the π mass are held constant at 1185 MeV and 137 MeV, respectively $(\delta_1 = \delta_4 = 1)$, and the couplings are left at the SU(3) degenerate values $(\epsilon_1 = \epsilon_2 = \cdots = \epsilon_5 = 0)$. When $\delta = 0$, all the decuplet masses coincide at 1.964 $(\text{BeV})^2$ or 1401 MeV. As δ increases, a mass splitting is induced in the decuplet. The masses are nearly equally spaced as is shown in the first line of Table 2, where we have given d_M as a function of δ. Figure 4 reveals the remarkable fact that although the mass of the decuplet as a function of the symmetry breaking is far from linear, equal spacing is well satisfied. Before discussing this situation, we examine some other examples of octet symmetry breaking.

In Fig. 5 we fix the baryon and meson masses at degenerate values $(\delta_1 = \delta_4 = 1, \ \delta_2 = \delta_3 = \delta_5 = 0)$ and vary the

symmetry breaking of the couplings. The example shown is typical. For some combinations of the ϵ's, equal spacing is retained to very large symmetry breaking. However, it is possible to find large enough ϵ's that the deviations from the average spacing are of order $\sim \frac{1}{2}$. In Fig. 5, $\epsilon = \epsilon_1 = \epsilon_2$ and $\epsilon_3 = \epsilon_4 = \epsilon_5 = 0$. Although the symmetry breaking is large enough that nonlinear effects are very noticeable, equal spacing is satisfied within 6% for $-0.2 < \epsilon < 0.05$. For $\epsilon > 0.05$, equal spacing becomes less well satisfied. As an example of very large symmetry breaking and very large deviations from equal spacing, we set $\epsilon = \epsilon_1 = \epsilon_2 = \epsilon_3 = \epsilon_4 = \epsilon_5$ and vary ϵ from -0.2 to 0.2. At $\epsilon = -0.2$, $d_M = 0.50$, and at $\epsilon = 0.2$, $d_M = 0.11$. Although the equal spacing of the decuplet is a remarkably stable result of octet symmetry breaking input, it is clear that the dynamics do not support octet symmetry breaking output indefinitely.

It is interesting to fix the baryon and meson masses at near the physical values and then vary the coupling constants. One might expect that superimposing large amounts of octet symmetry breaking in both the baryon masses <u>and</u> couplings should increase the violation of equal spacing of the decuplet masses. However, adding coupling constant perturbations to the mass perturbations often <u>improves</u> the equal mass spacing of the decuplet. As an example, consider Fig. 6, where we fix $\delta_1 = \delta_2 = \delta_3 = \delta_4 = \delta_5 = 1$ [baryon and meson masses near physical values--see Eq. (3.1)] and $\epsilon_3 = \epsilon_4 = \epsilon_5 = 0$. The parameter, $\epsilon = \epsilon_1 = \epsilon_2$, is varied, the decuplet masses are

plotted in Fig. 6, and the maximum deviation is given in the last
line of Table 2. Note that equal spacing is better satisfied for
$\epsilon = -0.1$ and $\epsilon = 0.2$ than it is for $\epsilon = 0$. Also, in Fig. 5
we saw for $\delta = \delta_2 = \delta_3 = \delta_5 = 0$ and $\epsilon = 0.2$, $d_M = 0.18$;
but when the mass splittings are turned on and $\delta = 1$ and $\epsilon = 0.2$,
then $d_M = 0.03$. Thus, the coupling and mass perturbations have
conspired to restore equal spacing.

In Fig. 7, we observe the evolution of these results by
setting $\epsilon = 0.2$ and turning on δ, i.e., $\epsilon_1 = \epsilon_2 = 0.20$,
$\epsilon_3 = \epsilon_4 = \epsilon_5 = 0$, $\delta_1 = \delta_4 = 1$, and $\delta = \delta_2 = \delta_3 = \delta_5$.
The large deviation from equal spacing at $\delta = 0$ dwindles to a
small symmetry breaking at $\delta = 1$. (See the second line of Table 2.)

In Figs. 5, 6, and 7, we have concentrated on the variable
$\epsilon = \epsilon_1 = \epsilon_2$. However, the qualitative results are quite general
and do not depend on the particular ϵ's we choose to vary. There
are many cases in which the baryon and meson masses and <u>couplings</u>
deviate from the pure symmetry values by large amounts, but the
decuplet satisfies equal spacing within a couple percent. Then, by
decreasing the symmetry breaking in the couplings, <u>larger</u> deviations
of the decuplet from equal spacing are obtained.

It is an amusing speculation to note that if the decuplet
spacings were actually equal within 1%, then this model would imply
large symmetry breaking of the baryon-meson couplings, $\gtrsim 15\%$. Of
course we cannot take this conclusion seriously since the experimental
errors on the spacing are about 5% (5% deviations are consistent with

no symmetry breaking in the baryon-meson couplings) and we have no accurate estimate of the theoretical errors.

We call attention to the nonlinearities apparent in Figs. 4 through 7. These might indicate that physical baryon and meson mass splittings represent a large symmetry breaking in the analysis of the decuplet mass spacings. However, many analyses are based on the first-order term of a perturbation expansion in the symmetry breaking, so it is worthwhile to examine the numerical accuracy of these theories. Again, we emphasize that the equal mass spacing of the decuplet is quite well satisfied in the exact solution to the model.

TABLE 2: Maximum Deviations of the Mass Spacings from the Average Spacing. The maximum deviation, d_M, is defined in Eq. (3.2). This table is a supplement to Figs. 4 through 7.

δ	0.01	0.04	0.09	0.16	0.25	0.36	0.49	0.64	0.81	1.00
$d_M(\epsilon = 0)$	0.002	0.009	0.020	0.019	0.015	0.016	0.017	0.025	0.033	0.040
$d_M(\epsilon = 0.2)$	0.183	0.144	0.090	0.034	0.009	0.023	0.033	0.028	0.030	0.031

ϵ	-0.20	-0.15	-0.10	-0.05	0.00	0.05	0.10	0.15	0.20	0.25	0.30
$d_M(\delta = 0)$	0.057	0.053	0.042	0.025	0.000	0.033	0.074	0.124	0.183	0.251	0.322
$d_M(\delta = 1)$	0.225	0.092	0.027	0.033	0.040	0.039	0.038	0.029	0.031	0.058	0.099

FIGURE CAPTIONS

Fig. 4. Decuplet Masses as Function of δ .

The baryon and meson mass parameters are $\delta_1 = \delta_4 = 1$ and

$\delta = \delta_2 = \delta_3 = \delta_5$. The coupling parameters are

$\epsilon_1 = \epsilon_2 = \epsilon_3 = \epsilon_4 = \epsilon_5 = 0$, $g = 19$, $f = 0.33$,

and $t = -1 \, (\text{BeV})^2$. The δ's and ϵ's are defined in

Eqs. (3.1) and (2.12), respectively. The lines labeled by

only the particle name represent the exact solution of the

model for the mass squared; the lines with D prefixed before

the particle name are the Dashen-Frautschi first-order mass

shifts, as discussed in Section V.

Fig. 5. Decuplet Masses as Function of ϵ .

The coupling parameter, $\epsilon = \epsilon_1 = \epsilon_2$, is varied. Set

parameters are $\epsilon_3 = \epsilon_4 = \epsilon_5 = 0$, $g = 19$, $f = 0.33$,

and $t = -1 \, (\text{BeV})^2$. The baryon and meson masses are SU(3)

degenerate, $\delta_1 = \delta_4 = 1$ and $\delta_2 = \delta_3 = \delta_5 = 0$.

Fig. 6. Decuplet Masses as Function of ϵ ; Symmetry Broken Baryon

and Meson Masses.

The coupling parameter, $\epsilon = \epsilon_1 = \epsilon_2$, is varied. Parameters

set at constant values are $\epsilon_3 = \epsilon_4 = \epsilon_5 = 0$, $g = 19$,

$f = 0.33$, and $t = -1 \, (\text{BeV})^2$. The baryon and meson masses

are set near the physical values, $\delta_1 = \delta_2 = \delta_3 = \delta_4 = \delta_5 = 1$.

Fig. 7. Decuplet Masses as Function of δ ; Symmetry Broken Baryon-

Meson Couplings.

The mass parameter, $\delta = \delta_2 = \delta_3 = \delta_5$, is varied, and $\delta_1 = \delta_4 = 1$. The coupling parameters are $\epsilon_1 = \epsilon_2 = 0.2$ and $\epsilon_3 = \epsilon_4 = \epsilon_5 = 0$. Also, $g = 19$, $f = 0.33$, and $t = -1 \ (\text{BeV})^2$.

Fig. 4
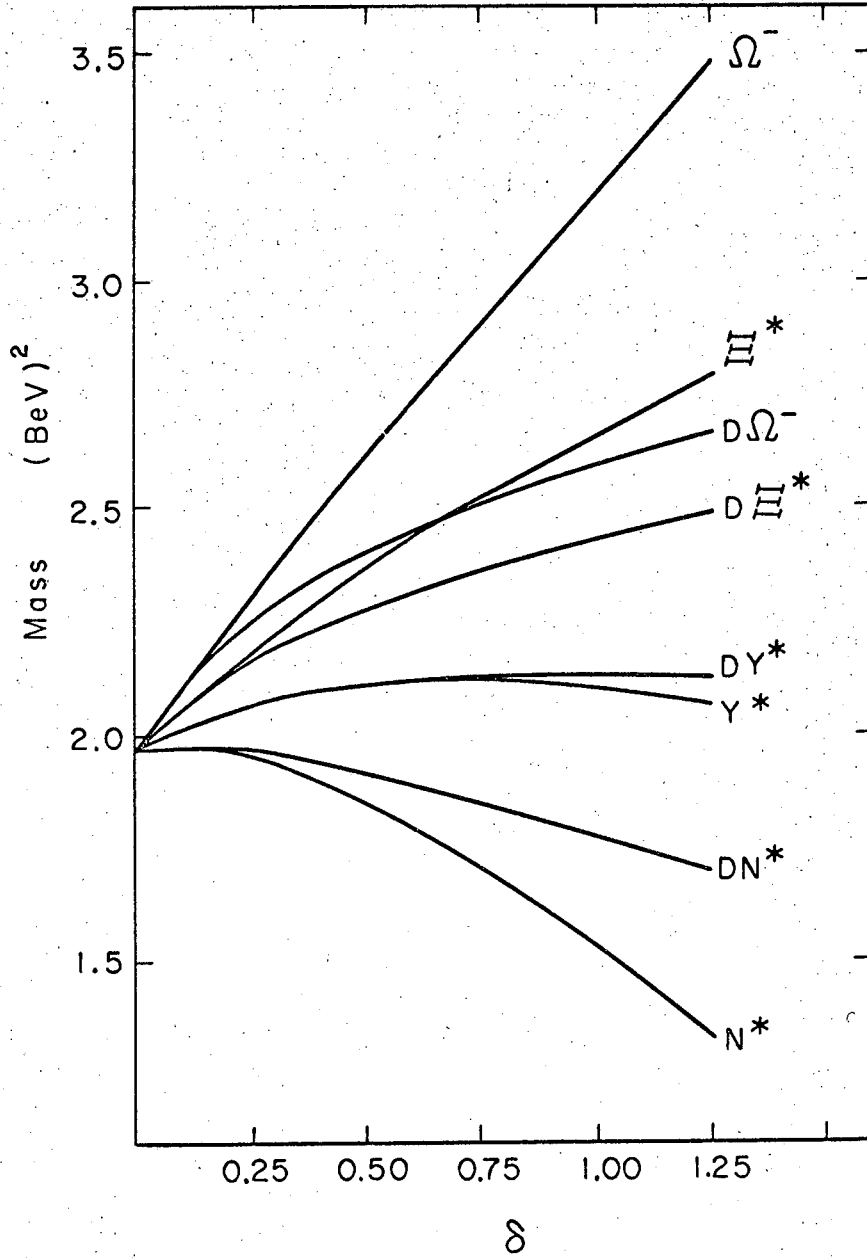
XBL673-2340

Fig. 5
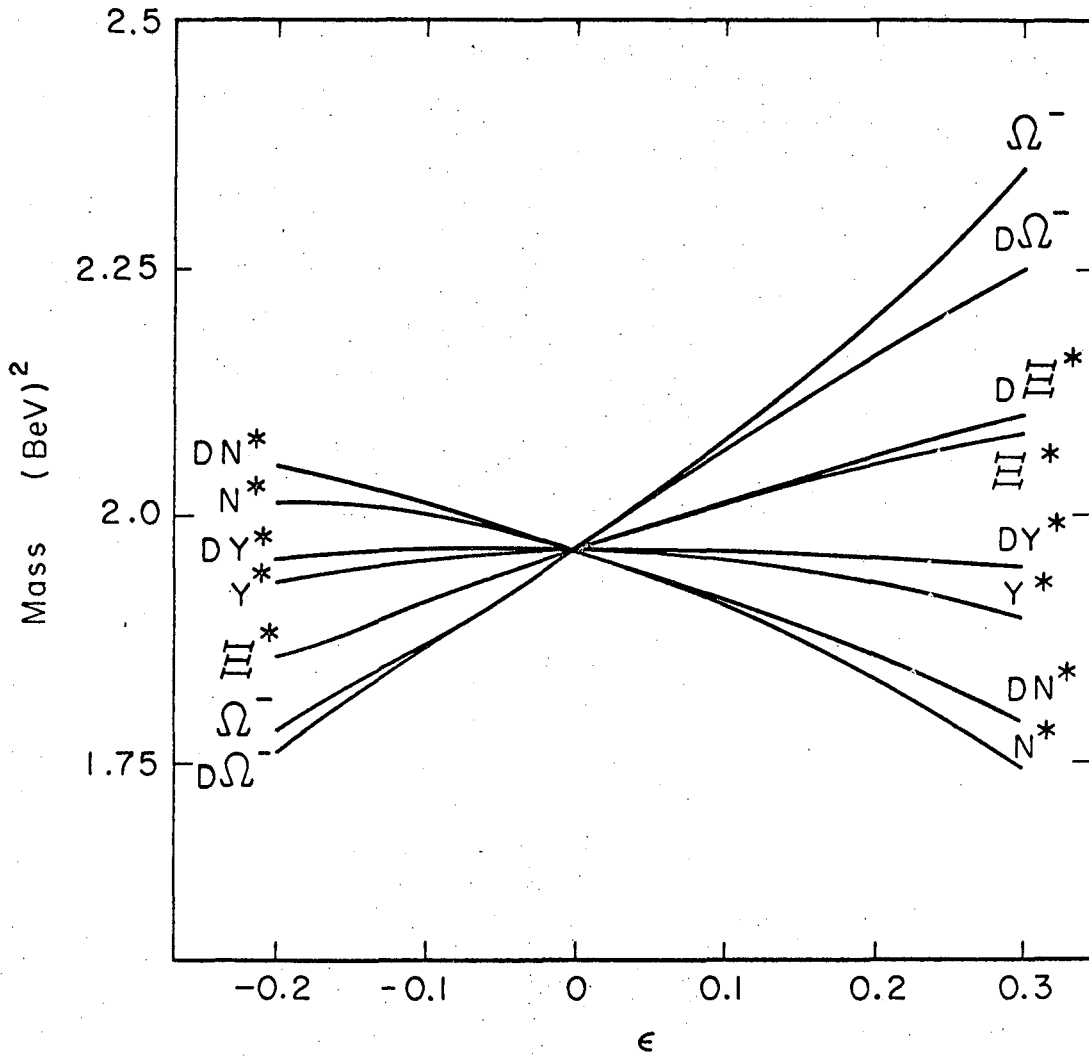
Fig. 6

XBL673-2342
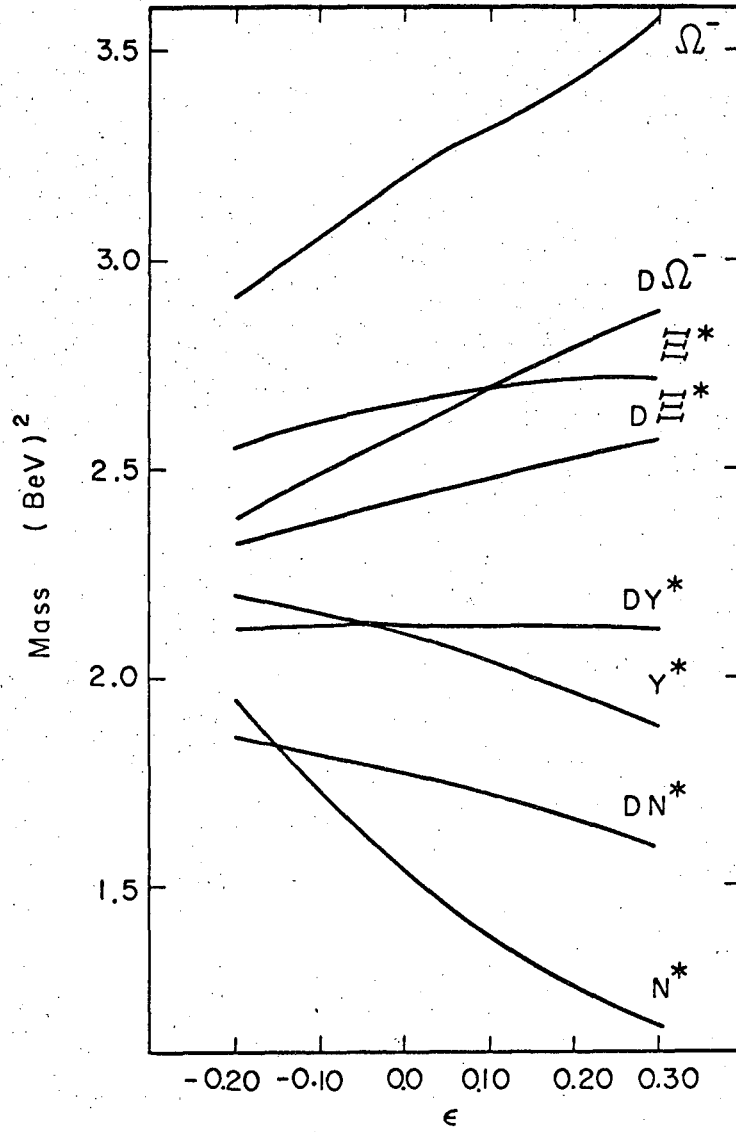
Fig. 7
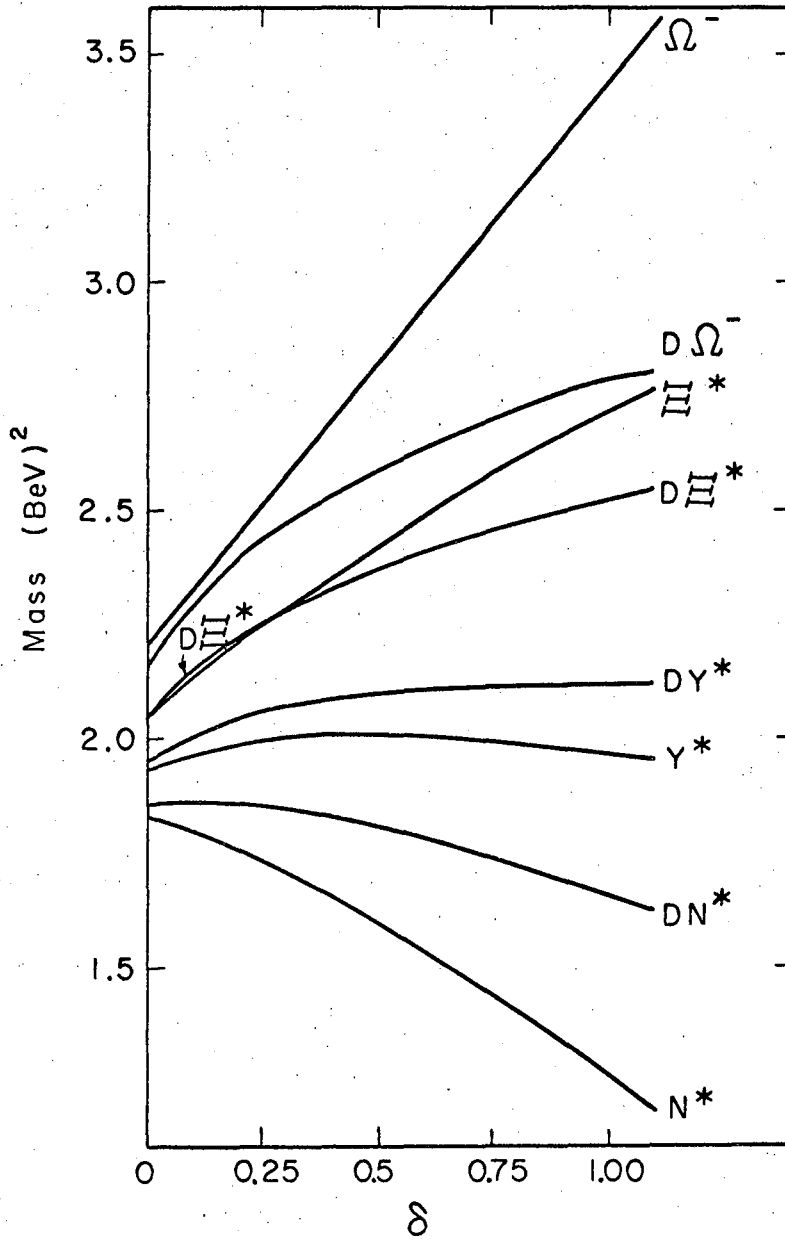
IV. PERTURBATION THEORY: MASS EXPANSIONS

Assuming that the decuplet is a baryon-meson bound state, we presented evidence in Section III that the decuplet-mass splitting induced by the physical baryon and meson masses is "large". The graphs of the decuplet masses as functions of the symmetry breaking are notably nonlinear; a linear approximation to Fig. 4 gives spacings which are much smaller than the exact solution. Also, we observed some amusing violations of the famous rule that octet symmetry-breaking input implies octet symmetry-breaking output to first order. These violations (see Figs. 4-7) cannot be explained by a first-order theory.

Nevertheless, many dynamical calculations of the decuplet analyze the $SU(3)$ symmetry breaking only in a first-order approximation.[4,7] This is a fruitful approach to the full dynamics, since many theoretical and practical difficulties are absent, and it is possible actually to obtain numerical results. However, because of the manifestations of higher-order contributions, we should check the numerical accuracy of these calculations.

Our model of the decuplet was solved exactly in Section III, and now we compare the numerical results of several perturbation formulas with those exact solutions. There are some rather important reasons for making these explicit numerical comparisions: (i) The comparisions can be used to define "large" symmetry breaking. If the exact and first-order results differ substantially for physical

baryon and meson masses, then it is possible that certain features of the physical symmetry breaking cannot be discovered from the first-order calculation. (ii) The reliability of linearized-perturbation bootstrap calculations depends on the numerical accuracy of the first-order approximations. For example, fitting the spacing of the decuplet with the free parameters in a first-order calculation might cause large distortions in the self-consistent baryon-meson (and decuplet) couplings, since the spacing is also sensitive to the symmetry breaking of the couplings. (iii) If the first-order results are very inaccurate, then it is likely that a second-order calculation will also be unreliable. This would suggest that perturbation theory is an awkward way to approach SU(3)-symmetry breaking in strong interactions. A crude second-order calculation checks this point.

We examine two possible perturbation theories. In this section, the $D(s)$ matrix is expanded in the mass splittings of the external baryons and mesons.[7] The expansion is simple and nonrigorous, but it should yield some understanding of the accuracy of low-order perturbation theory. In Section V, we consider the rigorous Dashen-Frautschi first-order theory.[8]

Each matrix element of $D(s)$ [Eq. (2.1)] is a function of the external baryon and meson masses of the initial channel. The most primitive possible perturbation theory consists of expanding the matrix elements, $D_{ij}(s, M_i^2, \mu_i^2)$, around $D(s, M_0^2, \mu_0^2)$, where M_0 and μ_0 are the degenerate baryon and meson masses. To simplify the notation, we define

$$D_{ij}(s, m_k^2) = D_{ij}(s, M_i^2, \mu_i^2) . \qquad (4.1)$$

The first- and second-order mass expansions of $D(s)$ are

$$D_{ij}^{(1)}(s, m_k^2) = D_{ij}(s, m_0^2) + \sum_k \left. \frac{\partial D(s, m_k^2)}{\partial m_k^2} \right|_{m_0^2} (m_k^2 - m_0^2) \qquad (4.2)$$

and

$$D_{ij}^{(2)}(s, m_k^2) = D_{ij}^{(1)}(s, m_k^2) + \frac{1}{2} \sum_{k, \ell} \left. \frac{\partial^2 D(s, m_k^2)}{\partial m_k^2 \partial m_\ell^2} \right|_{m_0^2} \qquad (4.3)$$

$$\times (m_k^2 - m_0^2)(m_\ell^2 - m_0^2) .$$

After expanding each matrix element of $D(s)$ according to Eqs. (4.2) and (4.3), we find the decuplet masses by solving

$$\det [\operatorname{Re} D^{(1,2)}(s_B)] = 0 . \qquad (4.4)$$

The derivatives of the $D(s)$ function in Eqs. (4.2) and (4.3) are evaluated in Appendix III. Also, there is a proof in Appendix III that the order of integration and differentiation may be interchanged for the first and second derivatives. However, the third derivatives do not exist and the expansion diverges term by term for third order and higher. In spite of this, we expect the first- and second-order

expansions to retain some quantitative validity. The first-order approximation, Eq. (4.2), should be as accurate as any other first-order theory, except in the case of the bound-state mass near the degenerate threshold. [The first derivative of $D(s)$ with respect to mass has a cusp at $s = (M_0 + \mu_0)^2$.] The second derivative of $D(s)$ with respect to mass is unbounded at $s = (M_0 + \mu_0)^2 = 1.769$ $(BeV)^2$, and consequently we expect inaccurate solutions to Eq. (4.4) for the bound-state mass near the degenerate threshold. In Fig. 4, the N^* mass did cross the degenerate threshold at $\delta \simeq 0.6$.

We limit discussion of numerical results to the situation described by Fig. 4. (In Section V, we use the Dashen-Frautschi approximation for investigating coupling shifts.) The coupling-constant perturbations are zero $(\epsilon_1 = \epsilon_2 = \epsilon_3 = \epsilon_4 = \epsilon_5 = 0)$, $g = 19$, $f = 0.33$, $t = -1$ $(BeV)^2$, and $\delta_1 = \delta_4 = 1$. [See Eq. (3.1).] The baryon and meson mass-splitting parameter is $\delta = \delta_2 = \delta_3 = \delta_5$. The results are given both in graph (Fig. 8) and table form (Table 3).

It is difficult to make general statements about Table 3, since different accuracy may be required of various calculations. But we can make the following comments.

For $\delta < 0.1$, the second-order calculation more accurately reproduces the exact solution than the first-order calculation does.

The equal spacing is retained within about 2% in both the first- and second-order theories for $\delta < 0.1$. This suggests that equal spacing is satisfied in the second-order theory. Of course

Eq. (4.3) does not imply that the decuplet-mass shift will be purely second order since the determinant, Eq. (4.4), is a polynomial in the mass splittings. For $\delta \geqslant 0.1$, an (inconsistent) inclusion of third- and higher-order effects is already becoming important numerically (except for the Ω^- mass). Thus, the slight breakdown of equal mass spacing for $\delta \gtrsim 0.25$ could well be due to the inconsistent inclusion of higher-order terms.

When δ reaches about 0.25, the second-order approximation is no longer more reliable than the first-order approximation, and when δ goes to 1, both the first- and second-order approximations are very unreliable. The inconsistent inclusion of higher-order effects in the det $\{Re[D(s)]\}$ = 0 condition should not disturb the numerical accuracy of the mass expansions too seriously. The bad behavior of the derivatives of $D(s)$ at $s = (M_0 + \mu_0)^2$ could cause all the second-order results to be shifted slightly upwards (especially the N^*). However, the expansions are already quite inaccurate for $\delta \approx 0.5$, and it is probable that any second-order calculation will be no more reliable than the first-order one for physical baryon and meson masses $(\delta \approx 1)$. In the sense that is necessary to go to very high-order perturbation theory to obtain reliable results, the physical symmetry breaking is large.

TABLE 3: Decuplet Masses As Function of δ. No prefix or a prefix of 1, 2, or D in front of the particle name denotes the exact solution, linear mass expansion, second-order mass expansion, or Dashen-Frautschi approximation to the model, respectively. Equation (3.2) defines d_M and we omit d_M for $\delta = 0.01$ because of round off error. The coupling perturbations are zero, $f = 0.33$, $t = -1$ $(BeV)^2$, $g = 19$, $\delta_1 = \delta_4 = 1$, and $\delta = \delta_2 = \delta_3 = \delta_5$. [See Eq. (3.1).]

δ	0.01	0.04	0.09	0.16	0.25	0.36	0.64	1.00
N^*	1.9645	1.9665	1.9699	1.9688	1.9505	1.9136	1.7734	1.5292
$1N^*$	1.9644	1.9658	1.9672	1.9671	1.9639	1.9560	1.9194	1.8489
$2N^*$	1.9644	1.9665	1.9702	1.9756	1.9820	1.9872	1.9738	1.8578
DN^*	1.9646	1.9670	1.9725	1.9754	1.9665	1.9472	1.8770	1.7698
Y^*	1.9687	1.9836	2.0087	2.0393	2.0663	2.0894	2.1162	2.1028
$1Y^*$	1.9686	1.9825	2.0040	2.0314	2.0624	2.0951	2.1588	2.2124
$2Y^*$	1.9687	1.9836	2.0092	2.0464	2.0953	2.1554	2.3044	2.4818
DY^*	1.9688	1.9843	2.0121	2.0399	2.0654	2.0871	2.1183	2.1290

(Table 3 continued)

δ	0.01	0.04	0.09	0.16	0.25	0.36	0.64	1.00
Ξ^*	1.9730	2.0004	2.0466	2.1088	2.1816	2.2645	2.4508	2.6586
$1\Xi^*$	1.9728	1.9989	2.0401	2.0934	2.1556	2.2237	2.3678	2.5106
$2\Xi^*$	1.9729	2.0004	2.0472	2.1141	2.2015	2.3097	2.5914	2.9729
$D\Xi^*$	1.9731	2.0016	2.0506	2.1075	2.1626	2.2180	2.3275	2.4282
Ω^-	1.9772	2.0173	2.0839	2.1767	2.2945	2.4357	2.7769	3.1904
$1\Omega^-$	1.9770	2.0153	2.0755	2.1532	2.2436	2.3420	2.5467	2.7428
$2\Omega^-$	1.9771	2.0171	2.0844	2.1793	2.3025	2.4548	2.8562	3.4202
$D\Omega^-$	1.9773	2.0190	2.0924	2.1701	2.2458	2.3204	2.4628	2.5916
d_M		0.0094	0.0196	0.0194	0.0151	0.0166	0.0252	0.0396
$1d_M$		0.0085	0.0202	0.0359	0.0563	0.0815	0.1451	0.2206
$2d_M$		0.0111	0.0248	0.0420	0.0602	0.0793	0.1238	0.1982
Dd_M		0.0026	0.0444	0.0415	0.1069	0.1773	0.3071	0.4035

FIGURE CAPTIONS

Fig. 8.   Graph of Table 3.

See the caption for Table 3 for values of parameters.

Fig. 8
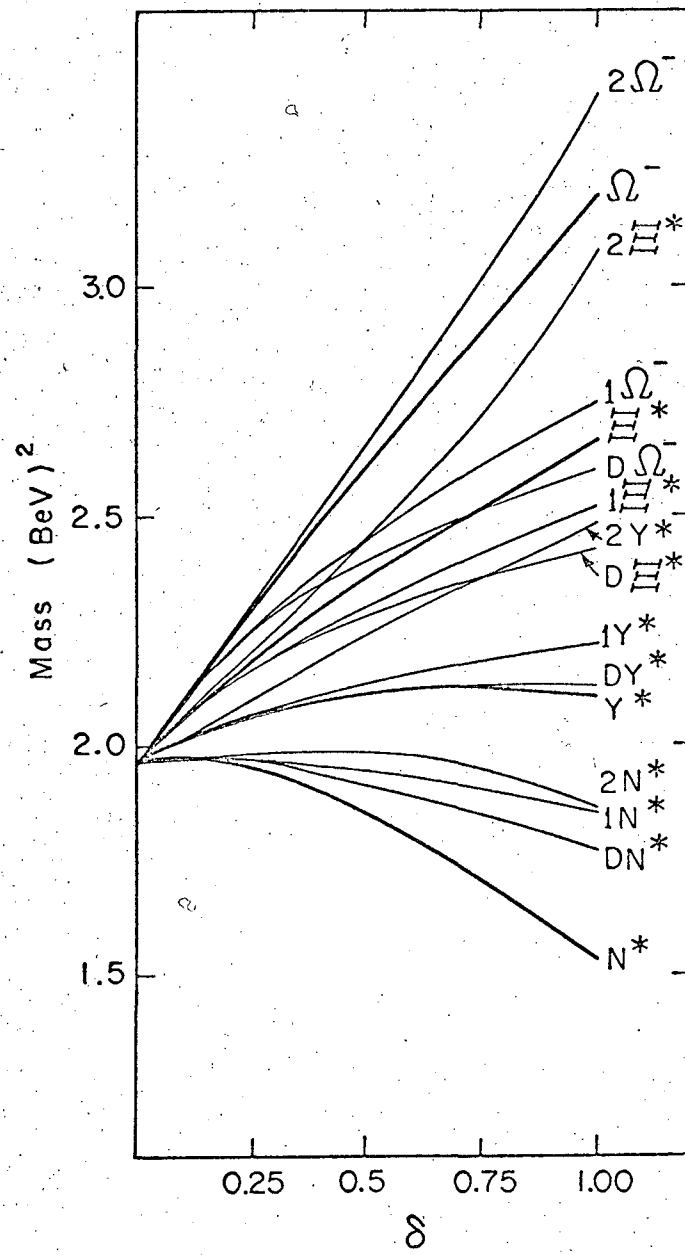
XBL673-2344

V. PERTURBATION THEORY: FIRST-ORDER DASHEN-FRAUTSCHI APPROXIMATION

The Dashen-Frautschi first-order mass-shift formula[8] has

provided a powerful method for studying strong and electromagnetic

mass shifts. Because of its popularity, it is certainly of interest

to examine the numerical accuracy of this approximation. In this

section, we compare the first-order results with the calculations of

Section III. Both the baryon and meson masses and couplings are

perturbed, and the induced decuplet mass shifts are computed directly

from the Dashen-Frautschi formula. This formula is convenient, since

it is not necessary to solve determinant equations such as Eq. (4.4).

Many objections to the mass expansion of Section IV do not

apply here. The mass expansion was termwise divergent for third order

and higher. However, the Dashen-Frautschi formula is the first term

of perturbation series. We discuss this in great detail in Part B,

where we derive an exact mass-shift formula. Here, we simply note

that there are no difficulties at the degenerate threshold, $s = (M_0 + \mu_0)^2$.

There are two practical difficulties with the expansion

associated with the Dashen-Frautschi formula. We find that the accuracy

of the first-order theory fails for symmetry breaking less than physical,

and so it would be useful to examine the second-order theory. The

second-order mass-shift formula [Part B, Eq. (4.8)] contains very

complicated dispersion integrals. We have not attempted to apply this

equation to this problem, but have relied on the less rigorous second-

order mass expansion for estimating the accuracy of second-order theories.

The second difficulty is rather trivial, but a discussion will aid the interpretation of our results. The Dashen-Frautschi theory is first-order in the changes of the left and right singularities, not the baryon and meson mass or coupling perturbations. Small changes of the right cuts are equivalent to small shifts in the baryon (and meson) masses. However, the baryon mass shifts are not linearly related to the changes of the right cuts. Thus, the simple group theoretical result, octet symmetry breaking of the input masses implies octet symmetry breaking in the output masses to first order in the input mass perturbations, does not apply to large baryon mass shifts. There is no obvious reason that the Dashen-Frautschi formula should give equal spacing for large baryon mass perturbations. In fact, for physical baryon and meson masses and no coupling perturbations, the Dashen-Frautschi theory gives deviations from equal spacing that are about 10 times those found in the exact solution. This result is probably not significant. However, the accuracy of the first-order mass shift is important.

The mass-shift formula is a result of the factorization theorem of the bound-state-pole residue. The first-order formula is most easily obtained by following the original derivation of Dashen and Frautschi in Ref. 8. We show how it follows from the exact mass-shift formula in the following paper. The first-order mass shift is

$$\delta s_B = - g_\Delta^T \; \tilde{N}^{-1}(s_B) \; w(s_B) \; N^{-1}(s_B) \; g_\Delta , \qquad (5.1a)$$

where

$$w(s) = \frac{1}{\pi} \int_L ds' \frac{\widetilde{D}(s') \, V'(s') \, D(s')}{s' - s} + \frac{1}{\pi} \int_R ds' \frac{\widetilde{N}(s') \, \delta\rho(s') \, N(s')}{s' - s} \, .$$

$$(5.1b)$$

The mass shift is δs_B ; s_B is the location of the bound-state pole with no symmetry breaking; $N(s)$ and $D(s)$ are calculated without symmetry breaking; $\delta\rho(s)$ is the change (due to the baryon and meson mass splittings) of the right discontinuities; V' is the change of the left discontinuities resulting from the symmetry breaking; and $g_{\Delta i}$ are the $SU(3)$-degenerate couplings of the decuplet to the baryon-meson channel.

In the pole approximation, the discontinuity across the left cuts is a matrix of constant coefficients times a delta function. The $N(s)$ matrix is simply

$$N(s) = B_0 \, (s - t)^{-1} \, , \qquad\qquad (5.2)$$

where t is the pole location and B_0 is (one of) the N_0 listed in Table 1 with $\epsilon_1 = \epsilon_2 = \epsilon_3 = \epsilon_4 = \epsilon_5 = 0$, i.e., $N(s)$ is $SU(3)$-symmetric.

The change of the left cuts is

$$B_0' = .N_0 - B_0 \, , \qquad\qquad (5.3)$$

where N_0 can include symmetry-broken couplings. With these simplifications, Eq. (5.1) becomes

$$\delta \, s_B \; = \; (t - s_B) \; \underset{\sim}{g}_\Delta^T \; w_1(s_B) \; \underset{\sim}{g}_\Delta \, , \qquad\qquad (5.4a)$$

where

$$w_1(s) \; = \; \tilde{B}_0^{-1} \, B_0' \, B_0^{-1} \; + \; \frac{s_B - t}{\pi} \; \text{P.V.} \int_R ds' \; \frac{\delta\rho(s')}{(s'- t)^2 (s'- s_B)} \, . \qquad (5.4b)$$

In the following calculations, we have defined the integral over the change of the right cuts to mean

$$\text{P.V.} \int_{(M+\mu)^2}^\infty ds' \; \frac{\rho(s')}{(s'- t)^2 (s'- s_B)} \; - \; \text{P.V.} \int_{(M_0+\mu_0)^2}^\infty ds' \; \frac{\rho_0(s')}{(s'- t)^2 (s'- s_B)} \qquad (5.5)$$

The couplings, $g_{\Delta i}$, are just the isoscalar factors for connecting a $\underset{\sim}{10}$ representation to the I and Y quantum numbers of the baryon and meson. An overall normalization (which is also the coupling of the Ω^- to the $\overline{K} \, \Xi$ channel) is

$$g_\Delta \; = \; \left[(s_B - t) \; \frac{\partial D}{\partial s} \Big|_{s = s_B} \right]^{-1/2} . \qquad\qquad (5.6)$$

The derivative was taken numerically in the following calculations. In units of g_Δ , decuplet couplings are

$$g(N^* N\pi) \; = \; -(2)^{-\frac{1}{2}} \, ,$$

$$g(N^* \Sigma K) \; = \; (2)^{-\frac{1}{2}} \, , \qquad\qquad (5.7)$$

$$g(Y^*N\overline{K}) \;=\; -(6)^{-\frac{1}{2}},$$

$$g(Y^*\,\Sigma\pi) \;=\; 6^{-\frac{1}{2}},$$

$$g(Y^*\Lambda\pi) \;=\; -\tfrac{1}{2},$$

$$g(Y^*\Xi K) \;=\; 6^{-\frac{1}{2}},$$

$$g(Y^*\Sigma\,\eta) \;=\; \tfrac{1}{2},$$

$$g(\Xi^*\,\Xi\,\pi) \;=\; \tfrac{1}{2},$$

$$g(\Xi^*\,\Lambda\,\overline{K}) \;=\; -\tfrac{1}{2},$$

$$g(\Xi^*\Sigma\,\overline{K}) \;=\; \tfrac{1}{2},$$

$$g(\Xi^*\,\Xi\,\eta) \;=\; \tfrac{1}{2},$$

$$g(\Omega^-\Xi\,\overline{K}) \;=\; 1.$$

The manipulations necessary to find the mass shifts from Eq. (5.4) were again performed on the IBM 1620 computer. Numerical comparison of this approximation with the exact solution of the model is shown in Figs. 4, 5, 6, and 7. In Table 4, we compare mass shifts for the case shown in Fig. 4 (no coupling perturbations); we note that the Dashen-Frautschi mass shifts are wrong by a factor of two for physical baryon

and meson masses. The mass expansions are compared with the Dashen-Frautschi approximation in Fig. 8 and Table 3. Some further comparisons are made in the next section.

TABLE 4: Comparison of Exact Mass Shifts with the Dashen-Frautschi Approximation as Function of δ . The coupling perturbations are zero, $f = 0.33$, $t = -1$ $(BeV)^2$, $g = 19$, $\delta_1 = \delta_4 = 1$, and $\delta = \delta_2 = \delta_3 = \delta_5$. The mass shift is in units of $(BeV)^2$. The prefix denotes the Dashen-Frautschi approximation; no prefix denotes the exact solution to the model.

δ	0.01	0.04	0.09	0.16	0.25	0.36	0.64	1.00
N^*	0.0007	0.0026	0.0061	0.0049	-0.0133	-0.0502	-0.1905	-0.4346
DN^*	0.0007	0.0031	0.0086	0.0116	0.0027	-0.0166	-0.0868	-0.1940
Y^*	0.0049	0.0197	0.0448	0.0755	0.1025	0.1256	0.1524	0.1390
DY^*	0.0050	0.0204	0.0483	0.0760	0.1016	0.1232	0.1544	0.1652
Ξ^*	0.0092	0.0366	0.0828	0.1449	0.2177	0.3007	0.4870	0.6948
$D\Xi^*$	0.0093	0.0377	0.0868	0.1436	0.1988	0.2542	0.3636	0.4644
Ω^-	0.0134	0.0534	0.1200	0.2129	0.3307	0.4718	0.8130	1.2266
$D\Omega^-$	0.0135	0.0551	0.1286	0.2063	0.2819	0.3565	0.4989	0.6278

VI. HEAVY BARYONS AND LINEAR APPROXIMATIONS

With a simple model, we have established that the 150 MeV mass spacing of the decuplet is not a small violation of SU(3) symmetry if the baryon-meson channels are most important in binding the decuplet. In spite of the nonlinearities, the model does give equal mass spacing, a result which the dynamics seem to favor independent of linear (or second order) perturbation theory. Even so, it is possible that the equal spacing of the decuplet is a first-order effect. We speculate about this possibility by considering baryon-meson channels in which the baryons are much more massive than the $J^P = \frac{1}{2}^+$ octet. Perhaps it is already clear that the physical spacings of the decuplet will be reached before the first-order formula breaks down if the baryons are sufficiently heavy.

This speculation is not completely idle since we have ignored all the higher mass channels that might help bind the decuplet. For example, if the $J^P = \frac{1}{2}^+$ octet lies on a Regge trajectory, then we might expect some contribution from the $J^P = \frac{5}{2}^+$ octet containing the $N_{\frac{1}{2}}(1688)$, and so on. We include the higher-mass channels in the following crude way. We assume that the incoming baryons transform as an octet, but that, averaged over all contributions, the baryons have a mass heavier than the usual $J^P = \frac{1}{2}^+$ octet; i.e., we increase δ_1 in Eq. (3.1). All decuplet meson channels are neglected. Thus, the model is exactly the same as that used in Section III, and it is solved in the same way. We then compare the exact solution of the model with the Dashen-Frautschi approximation.[8]

Suppose that the most important channels for binding the decuplet are composed of one baryon from the $J^P = \frac{5}{2}^+$ octet and one pseudoscalar meson. The thresholds are farther from the bound-state poles and the mass spacing of the $J^P = \frac{5}{2}^+$ is smaller than for the $J^P = \frac{1}{2}^+$ octet. Consequently, for physical $\frac{5}{2}^+$ baryon masses, the decuplet spacings are about one half the physical spacings. More precisely, we adjust g and t so that the N^* mass is 1236 MeV. Then for physical $\frac{1}{2}^+$ masses and $t = -1$ $(BeV)^2$, the spacing is 0.55 $(BeV)^2$. For the $\frac{5}{2}^+$ baryon masses, $t = -1$ $(BeV)^2$ implies a spacing of 0.20 $(BeV)^2$, $t = -3$ $(BeV)^2$ implies a spacing of 0.30 $(BeV)^2$, and $t = -5$ $(BeV)^2$ implies a spacing of 0.27 $(BeV)^2$. Since physical $J^P = \frac{1}{2}^+$ baryon masses and physical pseudoscalar-meson masses with SU(3) degenerate couplings lead to too large a spacing, it is possible that the higher mass-channel contributions reduce the spacing to its physical value.

We now show how the linear approximation is improved by increasing the baryon masses. In Fig. 9, we set $\delta_1 = 4$ so that the degenerate mass of the baryons is 2386 MeV. We also set $t = -7$ $(BeV)^2$, $g = 27.3$, $\epsilon_1 = \epsilon_2 = \epsilon_3 = \epsilon_4 = \epsilon_5 = 0$, and $\delta = \delta_2 = \delta_3 = \delta_5$. Note that for physical decuplet spacings, the Dashen-Frautschi approximation is beginning to fail.

If δ_1 is set equal to 9 (the degenerate mass is 3579 MeV) and the subtraction point put at -15 $(BeV)^2$, then the Dashen-Frautschi approximation is quite good when the physical decuplet spacing is reached, as is shown in Fig. 10.

FIGURE CAPTIONS

Fig. 9. The Decuplet Mass Splitting with Heavy Baryons.

The degenerate baryon mass is 2386 MeV. Also, $f = 0.33$,

$g = 27.3$, $t = -7$ $(\text{BeV})^2$, the coupling perturbations are

zero, $\delta_4 = 1$, $\delta_1 = 4$, and $\delta = \delta_2 = \delta_3 = \delta_5$. The

prefix D indicates that the Dashen-Frautschi approximation

was used in finding the mass shift; no prefix indicates the

exact solution of the model.

Fig.10. The Decuplet Mass Splitting with Very Heavy Baryons.

The degenerate baryon mass is 3579 MeV. Also, $f = 0.33$,

$g = 30.013$, $t = -15$ $(\text{BeV})^2$, the coupling perturbations

are zero, $\delta_4 = 1$, $\delta_1 = 9$, and $\delta = \delta_2 = \delta_3 = \delta_5$.

The prefix D indicates that the Dashen-Frautschi approximation

was used in finding the mass shift; no prefix indicates the

exact solution of the model.

Fig. 9
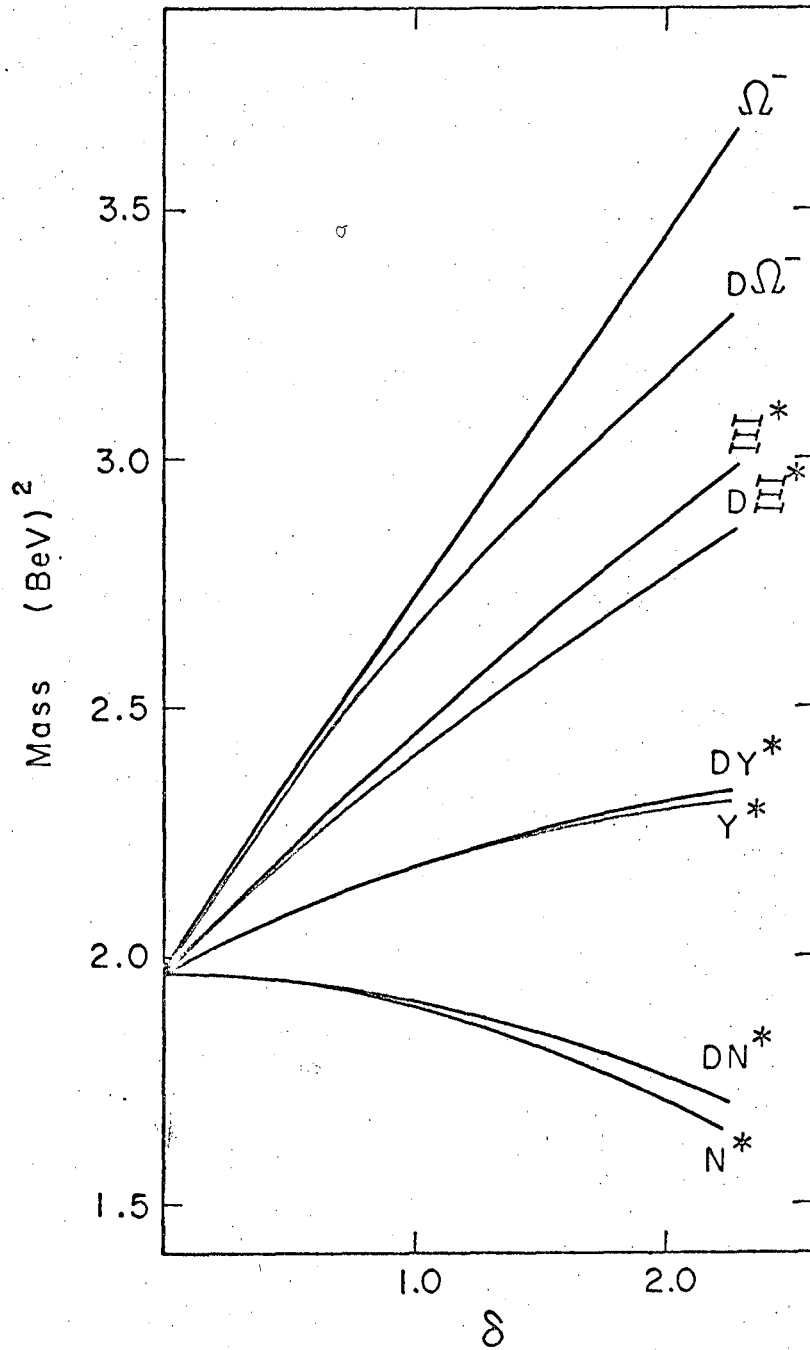
Fig. 10
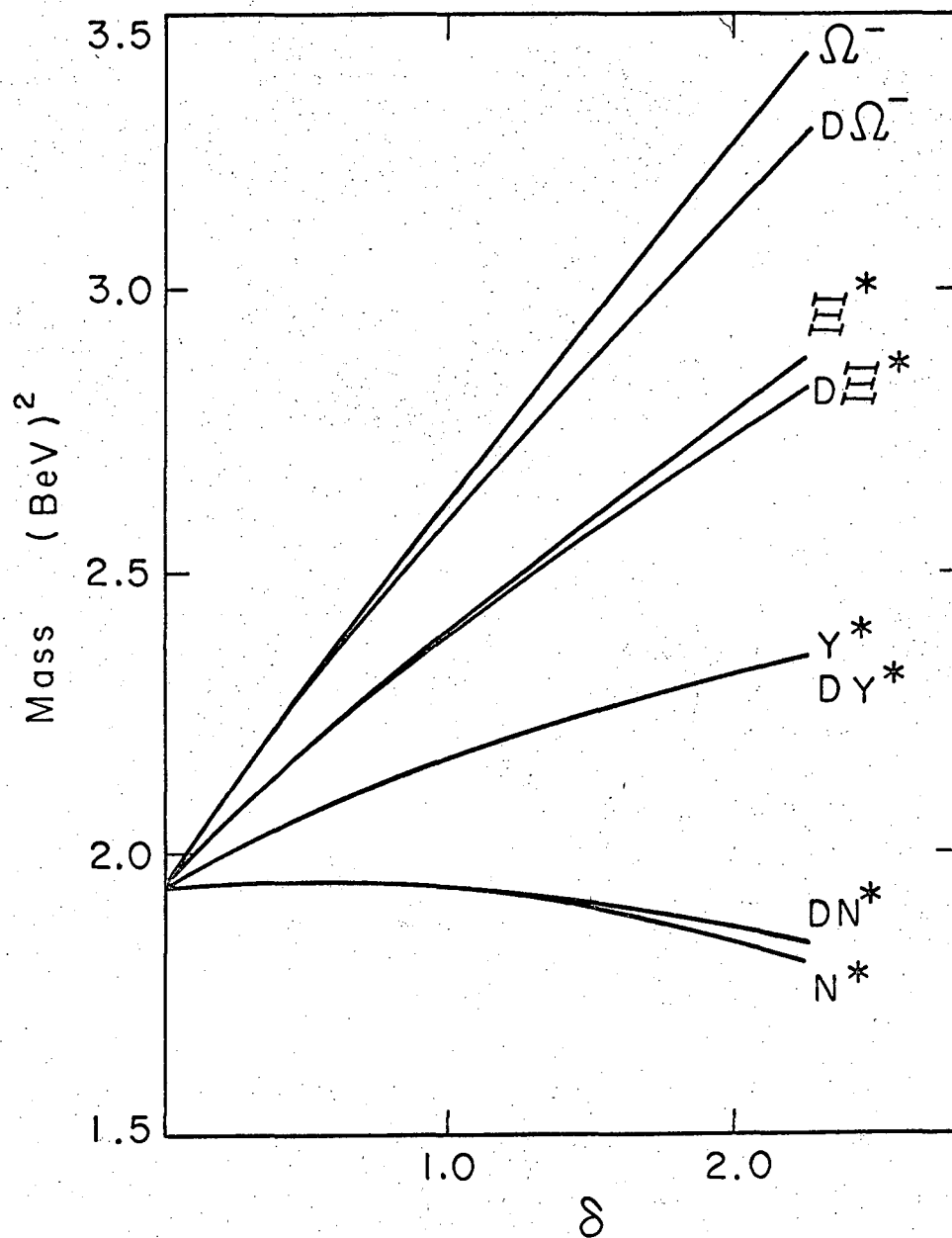
XBL673-2346

VII. AMPLITUDE OCTET SUM RULES

If the octet deviations from pure $SU(3)$ are small, then both the masses of bound states and the elements of the scattering amplitude satisfy octet sum rules. When the symmetry breaking parameters are large enough that the decuplet spacing approaches the physical value, the first-order approximations are poor and many manifestations of nonlinear behavior are obvious. Thus, the equal mass spacing of the decuplet is not explained by assuming that the symmetry breaking is small.

We do not know why the dynamics favor octet sum rules for the bound-state masses. But it is conceivable that the matrix elements of the transition operator also satisfy the octet sum rules, and that octet symmetry breaking is a general property that is rather independent of perturbation theory. However, the amplitude octet sum rules fail for about the same values of the symmetry-breaking parameters at which the first-order theories become inaccurate. We now discuss this quantitatively.

In Section III, we calculated the amplitudes for meson-baryon scattering for the values of I and Y that correspond to the decuplet quantum numbers. These four scattering matrices were written in a channel basis in which each matrix element was the amplitude for a transition from one meson-baryon state to another. To discuss the $SU(3)$ transformation properties of these amplitudes, it is convenient to transform to an $SU(3)$ basis. We then assume that the amplitude

transforms as an $SU(3)$ singlet plus the $I = 0$, $Y = 0$ member of an octet. A simple application of the Wigner-Eckhart Theorem for $SU(3)$ gives

$$(U^T A U)_{r\gamma, r'\gamma'} = \delta_{rr'} \delta_{\gamma\gamma'} a_{r\gamma} + \sum_\mu \begin{pmatrix} r' & 8 & | & r & \mu \\ \Delta & 0,0 & | & \Delta & \end{pmatrix} a_{r\gamma, r'\gamma'}^{(\mu)}.$$

(7.1)

This expression is very simple, although the multiplicity of $\underset{\sim}{8}$'s in $\underset{\sim}{8} \otimes \underset{\sim}{8}$ complicates the notation. The amplitude A is in the channel basis as calculated in Section III, and the matrix, U, which is a matrix of isoscalar factors, transforms A to the $SU(3)$ basis,

$$(U)_{ij, r\gamma} = \begin{pmatrix} 8 & 8 & | & r\gamma \\ I_i Y_i & I_j Y_j & | & \Delta \end{pmatrix},$$

(7.2)

where I_i and Y_i, and I_j and Y_j are the isospin and hypercharge of the baryon and meson in channel ij. The indices r and γ (r' and γ') denote the $SU(3)$ representation and the multiplicity, respectively (i.e., there are two $\underset{\sim}{8}$'s for the channels communicating with the Y^* and Ξ^*.) The first term on the right side of Eq. (7.1) is the $SU(3)$ singlet contribution. The Wigner-Eckhart Theorem factors the quantum numbers of the decuplet particle out of the arbitrary constant, $a_{r\gamma, r'\gamma'}^{(\mu)}$. The μ is the multiplicity index of $\underset{\sim}{r}$ in $\underset{\sim}{r'} \otimes \underset{\sim}{8}$, and Δ denotes I and Y of the decuplet particle.

The sum rules are derived in the usual way. For example, the $\underset{\sim\sim}{10}$ to $\underset{\sim\sim}{10}$ transition amplitude appears in all four scattering matrices.

Since there are two arbitrary constants, we find two sum rules.
Altogether, there are nine octet sum rules that an octet symmetry-
broken amplitude must satisfy. We define a set of nine symbols,
$\sigma_{r-r'\gamma'}^{(j)}$, which are zero for pure octet symmetry breaking. The
subscript, $r - r'\gamma'$, means the transition from representation r
to representation r', and as before γ' is the multiplicity
index of $\underset{\sim}{r}'$. (There are no sum rules for the $\underset{\sim}{8}$ to $\underset{\sim}{8}$ transitions
and the amplitude is always symmetric, so we only need one multiplicity
index.) The index, j, simply numbers the sum rule for those
transitions which have several sum rules. If $\sigma_{r-r'\gamma'}^{(j)}$ is set
equal to zero, these sum rules follow from Eq. (7.1):

$$s_c\ \sigma_{27-10}^{(1)} = A_{27-10}\ (Y^*) - (8/15)^{1/2}\ A_{27-10}\ (N^*)\ ,$$

$$s_c\ \sigma_{27-10}^{(2)} = A_{27-10}\ (\Xi^*) - (5)^{-1/2}\ A_{27-10}\ (N^*)\ ,$$

$$s_c\ \sigma_{27-8,1} = A_{27-8,1}\ (Y^*) - (2/3)^{1/2}\ A_{27-8,1}\ (\Xi^*)\ ,$$

$$s_c\ \sigma_{27-8,2} = A_{27-8,2}\ (Y^*) - (2/3)^{1/2}\ A_{27-8,2}\ (\Xi^*)\ ,$$

$$s_c\ \sigma_{10-10}^{(1)} = A_{10-10}\ (\Xi^*) - 2A_{10-10}\ (Y^*) + A_{10-10}\ (N^*)\ ,$$

$$s_c\ \sigma_{10-10}^{(2)} = A_{10-10}\ (\Omega^-) - 3\ A_{10-10}\ (Y^*) + 2\ A_{10-10}\ (N^*)\ ,$$

(Equation 7.3 continued)

$$s_c \ \sigma_{10\text{-}8,1} \ = \ A_{10\text{-}8,1} \ (\Xi^*) - A_{10\text{-}8,1} \ (Y^*) \ ;$$

$$s_c \ \sigma_{10\text{-}8,2} \ = \ A_{10\text{-}8,2} \ (\Xi^*) - A_{10\text{-}8,2} \ (Y^*);$$

$$s_c \ \sigma_{10\text{-}\overline{10}} \ = \ A_{10\text{-}\overline{10}} \ (Y^*) \ . \tag{7.3}$$

The amplitude $A_{r\text{-}r'\gamma'}(\Delta)$ is the transition amplitude between representations r and $r' \ \gamma'$, and the I and Y quantum numbers are again denoted by the decuplet particle symbol. The scale factor, s_c, is inserted to make $\sigma_{r\text{-}r'\gamma'}^{(j)}$ dimensionless.

In Section III, we calculated the determinant of $\text{Re}\{D(s)\}$ in the computation of the bound-state pole positions. This was equivalent to finding the pole positions in the Hermitian K matrix, and had the advantage of avoiding complex arithmetic. For the same reason, we assume that the K matrix satisfies the octet sum rules, where

$$K(s) \ = \ N(s) \ \{\text{Re} \ D(s)\}^{-1}. \tag{7.4}$$

The sum rules will not be valid for all values of s. For s near a bound-state pole, the sum rules can be violated arbitrarily. For example, if s is between the Y^* and Ξ^* masses, then $K_{10\text{-}10}(N^*)$ and $K_{10\text{-}10}(Y^*)$ are both negative and $K_{10\text{-}10}(\Xi^*)$ and $K_{10\text{-}10}(\Omega^-)$ are both positive. (This is true for symmetry breaking

where the decuplet masses are in their physical order.) Consequently, equal spacing of the amplitudes is impossible, even for very small symmetry breaking. [See Eq. (7.3).] Thus, we test the sum rules for values of s where $K(s)$ is a slowly-varying function. In our model, this is equivalent to avoiding s near pole positions, or

$$\max \{K_{r\gamma-r'\gamma'}(\Delta;s)\} \leq b ,$$

where b is a bound of order 1.

In applying this criterion to $K(s)$, it would seem natural to take s much larger than the decuplet masses. However, the K matrix has a set of poles where the phase shifts return through zero. For reasonably small symmetry breaking, these poles appear at $10 \; (\text{BeV})^2 \leq s \leq 15 \; (\text{BeV})^2$. We avoid all poles by choosing $b = 2$.

For symmetry breaking of order $\delta \lesssim 0.5$ (See Fig. 4), $K_{27-10}(\Delta)$ is from 5 to 10 times larger than the next largest off-diagonal K-matrix element in the $SU(3)$ basis. Also, the spacings of $K_{10-10}(\Delta)$ are of order $K_{27-10}(\Delta)$. If the scale factor is chosen to be of this magnitude, then the violations of the other sum rules will be "small". We let the scale factor be

$$s_c = \max \{ |K_{10-10}(Y^*) - K_{10-10}(N^*)|, \; |K_{10-10}(\Xi^*) - K_{10-10}(Y^*)| ,$$

$$\text{(7.5)}$$

$$|K_{10-10}(\Omega^-) - K_{10-10}(\Xi^*)| \} .$$

We evaluate the first two sum rules of Eq. (7.3) as they are, but discuss the $K_{10-10}(\Delta)$ spacings by a simple parameter, γ, which is the maximum deviation from the average spacing of the 10-10 amplitude,

$$s_c \gamma = s_c - 3^{-1} [K_{10-10}(\Omega^-) - K_{10-10}(N^*)] . \qquad (7.6)$$

Before examining the numerical details, we should emphasize that s_c is linear in the symmetry breaking to lowest order. Since the right side of Eq. (7.3) is already second-order in the symmetry-breaking (the octet sum rules are satisfied to first-order), it follows that the linear behavior of σ and γ corresponds to second order symmetry breaking effects and the curvature of the plots of σ and γ to higher-order effects.

In Fig. 11, we show σ and γ as functions of the meson and baryon mass splitting parameter, δ. The plots are remarkably linear out to $\delta = 0.7$. However, on closer examination we find that third-order effects and higher are important, even at $\delta = 0.7$. This is because a strong second-order effect in s_c cancels the strong third-order effect in, for example, $K_{27-10}(Y^*)$.

The importance of the higher-order effects becomes obvious when we plot σ and γ as functions of the coupling symmetry-breaking parameter, $\epsilon = \epsilon_1 = \epsilon_2$. Here, the second-order terms of s_c are of the same sign and magnitude as the third-order effects in, for example, $K_{27-10}(Y^*)$, and the plot is quite nonlinear, as shown in Fig. 12.

These results are not very dependent on the value of s , if s is not near a pole of $K(s)$. The sum rules slowly become better satisfied as s is increased. For example, if $\delta = 0.25$ and $\epsilon = 0$, then: $\gamma = 0.23$ at $s = 14 \ (\text{BeV})^2$; $\gamma = 0.10$ at $s = 20 \ (\text{BeV})^2$; and $\gamma = 0.04$ at $s = 45 \ (\text{BeV})^2$.

The symmetry breaking is large in the sense that first-order formulas are quite inaccurate. The second-order theory improves the situation only slightly, and when physical symmetry breaking is reached, it is as unreliable as the first-order theory. Finally, the octet symmetry breaking output is special to the bound-state pole positions; the amplitude does not satisfy the octet sum rules for physical symmetry breaking.

FIGURE CAPTIONS

Fig. 11. Violations of the Amplitude Octet Sum Rules as Function of δ.

The parameters are: $\alpha = \sigma_{27\text{-}10}^{(1)}$ [Eq. (7.3)]; $\beta = \sigma_{27\text{-}10}^{(2)}$;

and γ is defined in Eq. (7.6). Also, $f = 0.33$, $t = -1$ (BeV)^2,

$g = 19$, $s = 5$ (BeV)^2, $\delta_1 = \delta_4 = 0$, $\epsilon_1 = \epsilon_2 = \epsilon_3 = \epsilon_4 = \epsilon_5 = 0$,

and $\delta = \delta_2 = \delta_3 = \delta_5$.

Fig. 12. Violations of the Amplitude Octet Sum Rules as Function of ϵ..

The parameters are: $\alpha = \sigma_{27\text{-}10}^{(1)}$ [Eq. (7.3)]; $\beta = \sigma_{27\text{-}10}^{(2)}$;

and γ is defined in Eq. (7.6). Also, $f = 0.33$, $t = -1$ (BeV)^2,

$g = 19$, $s = 5$ (BeV)^2, $\delta_1 = \delta_4 = 1$, $\delta_2 = \delta_3 = \delta_5 = 0$,

$\epsilon_3 = \epsilon_4 = \epsilon_5 = 0$, and $\epsilon = \epsilon_1 = \epsilon_2$.

Fig. 11
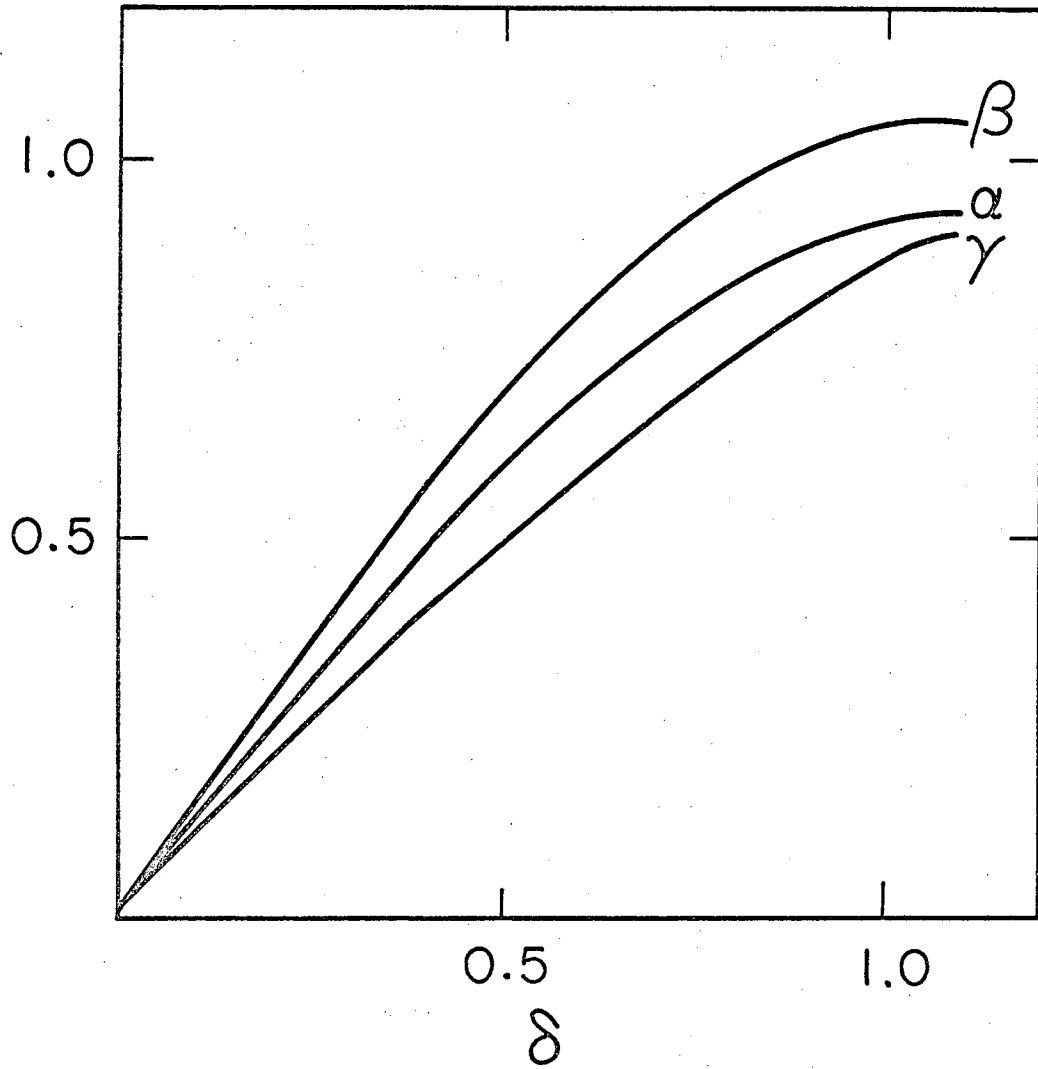
XBL673-2347

Fig. 12
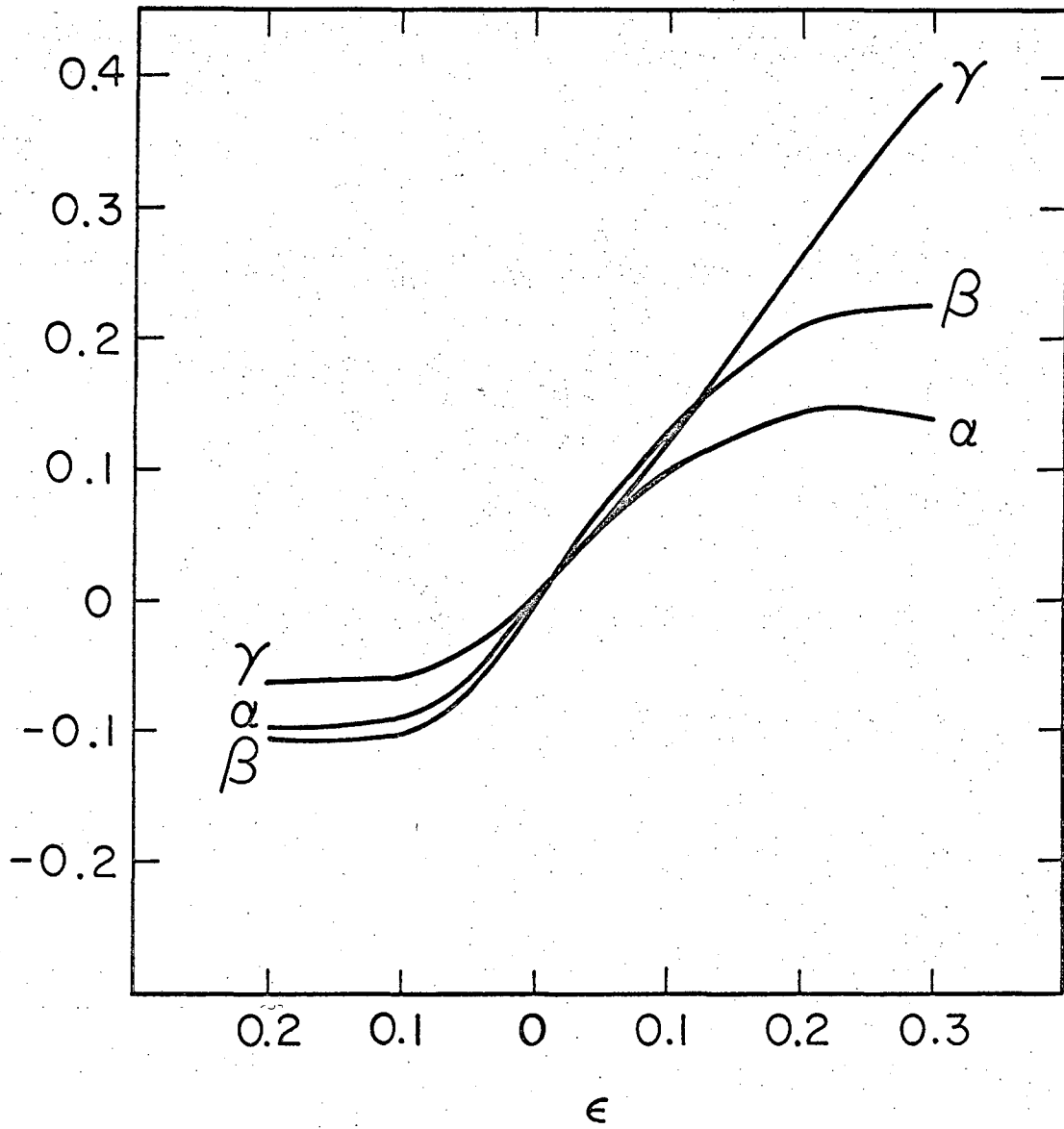
XBL 673-2348

ACKNOWLEDGMENTS

It is a great pleasure to acknowledge the guidance, advice, and suggestions of Professor Stanley Mandelstam. His encouragement and ideas have been very helpful.

I wish to thank Professor Howard Shugart for aid in using the computer. I am also grateful for conversations with Dr. John Harte, Dr. Victor Chung, and Mr. Daniel Finley.

I am especially grateful to Dr. Elliot Leader for his early guidance and continued interest in my work. This work was done under the auspices of the United States Atomic Energy Commission.

APPENDIX I: OCTET PERTURBATIONS OF THE BARYON-MESON COUPLING CONSTANTS

The eight baryons, the eight antibaryons, and the eight pseudoscalar mesons are assigned to eight-dimensional representations of $SU(3)$. In tensor notation, we symbolize the elements of the octet tensor by $T_a{}^b$, where $T_a{}^a = 0$. ($T_a{}^b$ is traceless.) A sum on repeated subscripts is implied, and a, b, etc. take on values $1,2,3$. We associate particles with tensor components by the prescription,

$$I_z = \tfrac{1}{2}\{n_u(2) + n_1(1) - n_1(2) - n_u(1)\} \qquad (A1.1)$$

and

$$Y = n_u(3) - n_\ell(3) + (j - k)/3 \,,$$

where

$$T = T_{a_1 \ldots a_j}{}^{b_1 \ldots b_k} \,,$$

and the symbols $n_u(i)$ and $n_1(j)$ denote the number of upper i's and the number of lower j's of the tensor component. The requirement of tracelessness with respect to $SU(3)$ and isotopic spin also gives some non-trivial normalization conditions. The usual identifications follow,

$$
(B_a{}^b) = \begin{pmatrix} \dfrac{\Sigma^0}{\sqrt{2}} - \dfrac{\Lambda}{\sqrt{6}} & \Sigma^+ & p \\[2ex] \Sigma^- & -\dfrac{\Sigma^0}{\sqrt{2}} - \dfrac{\Lambda}{\sqrt{6}} & n \\[2ex] \Xi^- & \Xi^0 & \dfrac{2}{\sqrt{6}}\Lambda \end{pmatrix}, \quad (A1.3)
$$

$$
(\bar{B}_a{}^b) = \begin{pmatrix} \dfrac{\bar{\Sigma}^0}{\sqrt{2}} - \dfrac{\bar{\Lambda}}{\sqrt{6}} & \bar{\Sigma}^+ & \bar{\Xi}^+ \\[2ex] \bar{\Sigma}^- & -\dfrac{\bar{\Sigma}^0}{\sqrt{2}} - \dfrac{\bar{\Lambda}}{\sqrt{6}} & \bar{\Xi}^0 \\[2ex] \bar{p} & \bar{n} & \dfrac{2}{\sqrt{6}}\bar{\Lambda} \end{pmatrix}
$$

$$
(P_a{}^b) \equiv (\bar{P}_a{}^b) = \begin{pmatrix} \dfrac{\pi^0}{\sqrt{2}} - \dfrac{\eta}{\sqrt{6}} & \pi^+ & K^+ \\[2ex] \pi^- & -\dfrac{\pi^0}{\sqrt{2}} - \dfrac{\eta}{\sqrt{6}} & K^0 \\[2ex] K^- & \bar{K}^0 & \dfrac{2}{\sqrt{6}}\eta \end{pmatrix}
$$

The derivation of Eq. (2.12) is analogous to the derivation of the Gell-Mann-Okubo mass formula. The most general Yukawa coupling is

$$
H_{int} = C_{bdg}{}^{ace}\, \bar{B}_a{}^b\, B_c{}^d\, P_e{}^g . \qquad (A1.4)
$$

We omit the γ_5 to shorten the notation. The representations contained in Eq. (A1.4) are those included in $\underset{\sim}{8} \otimes \underset{\sim}{8} \otimes \underset{\sim}{8}$. If

I and Y are conserved, H_{int} cannot contain any components belonging to non-self-conjugate representations, and the six $\underset{\sim}{27}$'s and the $\underset{\sim}{64}$ are eliminated by assuming that the symmetry breaking transforms as the $Y = 0$, $I = 0$ member of an <u>octet</u>. Thus, the two $\underset{\sim}{1}$'s and the eight $I = 0$, $Y = 0$ components of the eight $\underset{\sim}{8}$'s in Eq. (A1.4) are all that we need to consider. We write H_{int} as

$$2^{-\frac{1}{2}} H_{int} = g_D \, tr[\overline{B}(PB + BP)] + g_F \, [\overline{B}(PB - BP)]$$

$$+ C_1 (PB\overline{B})_3^{\;3} + C_2 (B\overline{B}P)_3^{\;3} + C_3 (\overline{B}PB)_3^{\;3}$$

$$\text{(A1.5)}$$

$$+ C_4 (BP\overline{B})_3^{\;3} + C_5 (\overline{B}BP)_3^{\;3} + C_6 (P\overline{B}B)_3^{\;3}$$

$$+ C_7 \, P_3^{\;3} \, tr(\overline{B}B) + C_8 \, B_3^{\;3} \, tr(\overline{B}P) + C_9 \, \overline{B}_3^{\;3} \, tr(BP) \; .$$

The C's cannot all be independent, since there are only eight $\underset{\sim}{8}$'s in $\underset{\sim}{8} \, \otimes \, \underset{\sim}{8} \, \otimes \, \underset{\sim}{8}$. But the product of three traceless matrices is not necessarily traceless, so we must subtract out the $\underset{\sim}{1}$ included in the last nine terms of Eq. (A1.5). Moreover, the hermiticity of H_{int} implies that $C_1 = C_2$, $C_5 = C_6$, and $C_8 = C_9$. This leaves five independent octet symmetry-breaking terms.

The relation that gives the linear dependence of the coefficients is[10]

$$(P B\bar{B} + B\bar{B}P + \bar{B}PB + BP\bar{B} + \bar{B}BP + P\bar{B}B)_3{}^3$$

$$- \text{tr}\,(\bar{B}BP) - \text{tr}\,(\bar{B}PB) = P_3{}^3\,\text{tr}\,(\bar{B}B) + B_3{}^3\,\text{tr}(\bar{B}P)$$

$$+ \bar{B}_3{}^3\ \text{tr}(BP). \tag{A1.6}$$

Equation (A1.6) is easily verified from Table A1.1, where the results of the necessary matrix multiplications are exhibited.

If $g_D = gd$, $g_F = gf$, and $d + f = 1$, then Eq. (A1.5) becomes

$$H_{int}\,/(g\sqrt{2}) = \text{tr}[\bar{B}(PB + BP)] - 2f\,\text{tr}(\bar{B}BP)$$

$$+ \epsilon_1{}' \, [PB\bar{B} + B\bar{B}P)_3{}^3 - (2/3)\,\text{tr}(\bar{B}PB)]$$

$$+ \epsilon_2{}' \, [(\bar{B}PB)_3{}^3 - \tfrac{1}{3}\,\text{tr}(\bar{B}PB)] + \epsilon_3{}' \, [(BP\bar{B})_3{}^3 - \tfrac{1}{3}\,\text{tr}(\bar{B}BP)]$$

$$+ \epsilon_4{}' \, P_3{}^3\,\text{tr}(\bar{B}B) + \epsilon_5{}' \, [B_3{}^3\,\text{tr}(\bar{B}P) + \bar{B}_3{}^3\,\text{tr}(BP)]. \tag{A1.7}$$

We have used Eq. (A1.6) to eliminate the term proportional to $[(\bar{B}BP + P\bar{B}B)_3{}^3 - (2/3)\,\text{tr}(\bar{B}BP)]$. To obtain the simple parameterization of the coupling perturbations of Eq. (4.7), let

$$\epsilon_1{}' = -\epsilon_1 + \epsilon_2 + \epsilon_3$$

$$\epsilon_2{}' = \epsilon_2 + \epsilon_3$$

$$\epsilon_3{}' = \epsilon_3.$$

$$\epsilon_4{}' = \frac{1}{3}\epsilon_1 - \frac{1}{2}\epsilon_2 - \frac{2}{3}\epsilon_3 + \epsilon_4$$

$$\epsilon_5{}' = \frac{1}{3}\epsilon_1 - \frac{1}{2}\epsilon_2 - \frac{2}{3}\epsilon_3 + \epsilon_5 . \tag{A1.8}$$

Substituting Eq. (A1.8) into Eq. (A1.7), we compare the following two forms of H_{int} to derive Eq. (2.12),

$$H_{int}/(g\sqrt{2}) = tr[\bar{B}(PB + BP)] - 2f\ tr(\bar{B}BP)$$

$$+ \epsilon_1[(2/3)\ tr(\bar{B}PB) - (PB\bar{B} + B\bar{B}P)_3{}^3 + (1/3)\ B_3{}^3\ tr(\bar{B}P)$$

$$+ (1/3)\ \bar{B}_3{}^3\ tr(BP) + (1/3)\ P_3{}^3\ tr(\bar{B}B)]$$

$$+ \epsilon_2[-tr(\bar{B}PB) + (PB\bar{B} + B\bar{B}P)_3{}^3 + (\bar{B}PB)_3{}^3$$

$$-\frac{1}{2}\ B_3{}^3\ tr(\bar{B}P) - \frac{1}{2}\ \bar{B}_3{}^3\ tr(BP) - \frac{1}{2}\ P_3{}^3\ tr(\bar{B}B)]$$

$$+ \epsilon_\cdot$$

<div align="right">Equation (A1.9) continued</div>

$$+ \epsilon_3 \{ - \text{tr}(\overline{B}PB) - \frac{1}{3} \text{tr}(\overline{B}BP) + (PB\overline{B} + B\overline{B}P)_3^{\;3}$$

$$+ (\overline{B}PB)_3^{\;3} + (BP\overline{B})_3^{\;3} - (2/3) [B_3^{\;3} \text{tr}(\overline{B}P) + \overline{B}_3^{\;3} \text{tr}(BP) + P_3^{\;3} \text{tr}(\overline{B}B)] \}$$

$$+ \epsilon_4 P_3^{\;3} \text{tr}(\overline{B}B) + \epsilon_5 [B_3^{\;3} \text{tr}(\overline{B}P) + \overline{B}_3^{\;3} \text{tr}(BP)]$$

$$= g_{NN\pi} \; \overline{N} \; \underset{\sim}{\tau} \cdot \underset{\sim}{\pi} \; N - g_{\Lambda\Sigma\pi} (\overline{\Lambda} \; \underset{\sim}{\Sigma} \cdot \underset{\sim}{\pi} + \Lambda \; \underset{\sim}{\overline{\Sigma}} \cdot \underset{\sim}{\pi})$$

$$+ g_{\Sigma\Sigma\pi} \; i \; \underset{\sim}{\overline{\Sigma}} \cdot \underset{\sim}{\pi} \times \underset{\sim}{\Sigma} - g_{\Xi\Xi\pi} \Xi \; \underset{\sim}{\tau} \cdot \underset{\sim}{\pi} \; \Xi - g_{N\Lambda K} (\overline{\Lambda} \; \overline{K} \; N + \overline{N} \; K \; \Lambda)$$

$$+ g_{N\Sigma K} (\overline{N} \; \underset{\sim}{\tau} \cdot \underset{\sim}{\Sigma} \; K + \overline{K} \; \underset{\sim}{\tau} \cdot \underset{\sim}{\Sigma} \; N) - g_{\Lambda\Xi K} (\overline{\Lambda} \; \Xi \; K + \Lambda \; \overline{K} \; \overline{\Xi})$$

$$- g_{\Sigma\Xi K} (\overline{K} \; \underset{\sim}{\tau} \cdot \underset{\sim}{\Sigma} \; \overline{\Xi} + \Xi \; \underset{\sim}{\tau} \cdot \underset{\sim}{\Sigma} \; K) - g_{NN\eta} \; \overline{N}N\eta - g_{\Lambda\Lambda\eta} \; \overline{\Lambda} \; \Lambda \; \eta$$

$$- g_{\Sigma\Sigma\eta} \; \underset{\sim}{\overline{\Sigma}} \cdot \underset{\sim}{\Sigma} \; \eta - g_{\Xi\Xi\eta} \; \Xi \; \overline{\Xi} \; \eta \; . \tag{A1.9}$$

Table A1.1 aids in the comparision of the two forms of Eq. (A1.9).
The twelve isotopic spin invariant couplings are written out in
Table A1.2.

TABLE A1.1: Decomposition of the Singlet and Octet Couplings Into the Isotopic-Spin-Invariant

Couplings. Each SU(3) term is a sum of isotopic-spin couplings with the coefficients shown in

the table.

	$\bar{N}\tau\cdot\pi N$	$\bar{\Lambda}\Sigma\cdot\pi$ $+\Lambda\bar{\Sigma}\cdot\pi$	$i\bar{\Sigma}\cdot\pi$ $\times\Sigma$	$\Xi\tau\cdot\pi\Xi$	$\bar{\Lambda}\bar{K}N$ $+\Lambda\bar{N}K$	$\bar{N}\tau\cdot\Sigma K$ $+\bar{K}\tau\cdot\bar{\Sigma}N$	$\bar{\Lambda}\Xi K$ $+\Lambda\bar{K}\Xi$	$\bar{K}\tau\cdot\bar{\Sigma}\Xi$ $+\Xi\tau\cdot\bar{\Sigma}K$	$\bar{N}N\eta$	$\bar{\Lambda}\Lambda\eta$	$\bar{\Sigma}\cdot\Sigma\eta$	$\bar{\Xi}\Xi\eta$
$\sqrt{2}\ tr(\bar{B}PB)$	1	$-1/\sqrt{3}$	1	0	$2/\sqrt{3}$	0	$-1/\sqrt{3}$	1	$-1/\sqrt{3}$	$1/\sqrt{3}$	$-1/\sqrt{3}$	$2/\sqrt{3}$
$\sqrt{2}\ tr(\bar{B}BP)$	0	$-1/\sqrt{3}$	-1	1	$-1/\sqrt{3}$	1	$2/\sqrt{3}$	0	$2/\sqrt{3}$	$1/\sqrt{3}$	$-1/\sqrt{3}$	$-1/\sqrt{3}$
$\sqrt{2}\ (PB\bar{B} + \bar{B}BP)_3^3$	0	0	0	0	$2/\sqrt{3}$	0	$-1/\sqrt{3}$	1	0	$8/3\sqrt{3}$	0	$4/\sqrt{3}$
$\sqrt{2}\ (\bar{B}PB)_3^3$	1	0	0	0	$2/\sqrt{3}$	0	0	0	$-1/\sqrt{3}$	$4/3\sqrt{3}$	0	0
$\sqrt{2}\ (BP\bar{B})_3^3$	0	0	0	1	0	0	$2/\sqrt{3}$	0	0	$4/3\sqrt{3}$	0	$-1/\sqrt{3}$
$\sqrt{2}\left(B_3^3 tr(\bar{B}P) +\bar{B}_3^3 tr(BP)\right)$	0	$2/\sqrt{3}$	0	0	$2/\sqrt{3}$	0	$2/\sqrt{3}$	0	0	$4/\sqrt{3}$	0	0
$\sqrt{2}\ P_3^3\ tr(\bar{B}B)$	0	0	0	0	0	0	0	0	$2/\sqrt{3}$	$2/\sqrt{3}$	$2/\sqrt{3}$	$2/\sqrt{3}$
$\sqrt{2}\ tr[\bar{B}(PB+BP)]$	1	$-2/\sqrt{3}$	0	1	$1/\sqrt{3}$	1	$1/\sqrt{3}$	1	$1/\sqrt{3}$	$2/\sqrt{3}$	$-2/\sqrt{3}$	$1/\sqrt{3}$
$\sqrt{2}\ tr[\bar{B}(PB-BP)]$	1	0	2	-1	$\sqrt{3}$	-1	$-\sqrt{3}$	1	$-\sqrt{3}$	0	0	$\sqrt{3}$
$\sqrt{2}\ (\bar{B}BP+P\bar{B}B)_3^3$	0	0	0	0	$-1/\sqrt{3}$	1	$2/\sqrt{3}$	0	$4/\sqrt{3}$	$8/3\sqrt{3}$	0	0

TABLE A1.2: Decomposition of the Isotopic-Spin-Invariant Couplings.

$$\bar{N}\, \underset{\sim}{\tau}\cdot\underset{\sim}{\pi}\, N \;=\; \sqrt{2}\;\; \bar{p}\, n\, \pi^{+} + \sqrt{2}\;\; p\, \bar{n}\, \pi^{-} + (\bar{p}p - \bar{n}n)\pi^{0}$$

$$\bar{\Lambda}\, \underset{\sim}{\Sigma}\cdot\underset{\sim}{\pi} + \bar{\Lambda}\, \underset{\sim}{\bar{\Sigma}}\cdot\underset{\sim}{\pi} \;=\; \bar{\Lambda}\, \Sigma^{+}\pi^{-} + \bar{\Lambda}\, \Sigma^{0}\pi^{0} + \bar{\Lambda}\, \Sigma^{-}\pi^{+} + \Lambda\, \bar{\Sigma}^{+}\pi^{-} + \Lambda\, \bar{\Sigma}^{0}\pi^{0} + \Lambda\, \bar{\Sigma}^{-}\pi^{+}$$

$$i\, \underset{\sim}{\bar{\Sigma}}\cdot\underset{\sim}{\pi}\times\underset{\sim}{\Sigma} \;=\; \bar{\Sigma}^{+}(\Sigma^{0}\pi^{-} - \Sigma^{-}\pi^{0}) + \bar{\Sigma}^{0}(\Sigma^{-}\pi^{+} - \Sigma^{+}\pi^{-}) + \bar{\Sigma}^{-}(\Sigma^{+}\pi^{0} - \Sigma^{0}\pi^{+})$$

$$\Xi\, \underset{\sim}{\tau}\cdot\underset{\sim}{\pi}\, \bar{\Xi} \;=\; \sqrt{2}\; \bar{\Xi}^{0}\, \Xi^{-}\pi^{+} + \sqrt{2}\; \bar{\Xi}^{+}\, \Xi^{0}\pi^{-} + (\Xi^{-}\bar{\Xi}^{+} - \Xi^{0}\bar{\Xi}^{0})\pi^{0}$$

$$\bar{\Lambda}\, \bar{K}\, N + \Lambda\, \bar{N}\, K \;=\; \bar{\Lambda}\, p\, K^{-} + \bar{\Lambda}\, n\, K^{0} + \bar{p}\, \Lambda\, K^{+} + \bar{n}\, \Lambda\, K^{0}$$

$$\bar{N}\, \underset{\sim}{\tau}\cdot\underset{\sim}{\Sigma}\, K + \bar{K}\, \underset{\sim}{\tau}\cdot\underset{\sim}{\bar{\Sigma}}\, N \;=\; \bar{p}\, \Sigma^{0}K^{+} + \sqrt{2}\; \bar{p}\, \Sigma^{+}K^{0} + \sqrt{2}\; \bar{n}\, \Sigma^{-}K^{+} - \bar{n}\, \Sigma^{0}K^{0} + \bar{\Sigma}^{0}p\, K^{-}$$
$$+ \sqrt{2}\; \bar{\Sigma}^{+}n\, K^{-} + \sqrt{2}\; \bar{\Sigma}^{-}p\, \bar{K}^{0} - \bar{\Sigma}^{0}n\, \bar{K}^{0}$$

$$\bar{\Lambda}\, \Xi\, K + \Lambda\, \bar{K}\, \bar{\Xi} \;=\; \bar{\Lambda}\, \Xi^{-}K^{+} + \bar{\Lambda}\, \Xi^{0}K^{0} + \bar{\Xi}^{+}\Lambda\, K^{-} + \bar{\Xi}^{0}\Lambda\, \bar{K}^{0}$$

$$\bar{K}\, \underset{\sim}{\tau}\cdot\underset{\sim}{\Sigma}\, \bar{\Xi} + \Xi\, \underset{\sim}{\tau}\cdot\underset{\sim}{\bar{\Sigma}}\, K \;=\; \bar{\Xi}^{+}\Sigma^{0}K^{-} + \sqrt{2}\; \bar{\Xi}^{+}\Sigma^{-}\bar{K}^{0} + \sqrt{2}\; \bar{\Xi}^{0}\Sigma^{+}K^{-} - \bar{\Xi}^{0}\bar{K}^{0}\Sigma^{0}$$
$$+ \bar{\Sigma}^{0}\Xi^{-}K^{+} + \sqrt{2}\; \bar{\Sigma}^{+}\Xi^{-}K^{0} + \sqrt{2}\; \bar{\Sigma}^{-}\Xi^{0}K^{+} - \bar{\Sigma}^{0}\Xi^{0}K^{0}$$

$$\bar{N}\, N\, \eta \;=\; \bar{p}\, p\, \eta + \bar{n}\, n\, \eta$$

$$\bar{\Lambda}\, \Lambda\, \eta \;=\; \bar{\Lambda}\, \Lambda\, \eta$$

(Table A1.2 continued)

$$\overline{\underset{\sim}{\Sigma}} \cdot \underset{\sim}{\Sigma} \, \eta \; = \; \overline{\Sigma}^+ \Sigma^- \, \eta \; + \; \overline{\Sigma}^0 \, \Sigma^0 \, \eta \; + \; \overline{\Sigma}^- \, \Sigma^+ \, \eta$$

$$\overline{\Xi} \, \overline{\Xi} \, \eta \; = \; \overline{\Xi}^+ \Xi^- \, \eta \; + \; \overline{\Xi}^0 \; \Xi^0 \, \eta$$

APPENDIX II: ISOSPIN CROSSING MATRICES

Although the derivation of the isospin crossing matrices is rather elementary in principle, it has been plagued with phase convention difficulties. In extending an appendix to a paper by Mandelstam et. al.,[13] Carruthers and Krisch[11] proposed to overcome the confusion by explicitly displaying the particle-state phase conventions in the field operators. In this formalism, there is a neat separation between the phase conventions for the particle states and the conventions related to the group theory of SU(2). The Condon and Shortley phase conventions place some restrictions on the phases in the field operators, but they do not determine the overall phase of the creation operators relative to the annihilation operators in the field operators. The phase choices of Carruthers and Krisch do not agree with those taken by de Swart[12] in his calculation of the vector coupling coefficients for SU(3). Since we use the de Swart isoscalar factors on several occasions (see Sections V and VII), it is mandatory that we follow his conventions. In our derivation of the isospin crossing matrices, we follow the general method of Carruthers and Krisch, but completely redo their phase convention discussion. We restrict our discussion to the u-channel to s-channel crossing matrices.

The s and u channels are defined by

$$a + b \rightarrow c + d \quad (s)$$

$$a + \bar{d} \rightarrow c + \bar{b} \quad (u)$$

(A2.1)

where b and d are pseudoscalar mesons and a and c are baryons.
The letters, a, b, c, and d, also denote the isospin of the particles,
and α, β, γ, and δ label the third component. The antiparticles of
a, b, c, and d are denoted by $\bar{a}$, $\bar{b}$, $\bar{c}$, and $\bar{d}$, and have third
components $-\alpha$, $-\beta$, $-\gamma$, and $-\delta$, respectively.

The continuation of the u-channel amplitude to the s-channel
physical region yields

$$\langle cd \,|M^s|\, ab \rangle \;=\; \xi_{su} \langle c\bar{b} \,|M^u|\, a\bar{d} \rangle . \qquad (A2.2)$$

After transforming to amplitudes of definite isospin (isospin
conservation is assumed here), we solve for $M^s(s')$, the s-channel
amplitude with isospin s' . A useful relation is

$$C(adu;\, \alpha,\, -\delta)\, C(cbu;\, \gamma,\, -\beta) \;=\; \sum_s \,(2u+1)\,(-1)^{b+d+\alpha+\gamma} \; x$$

$$\qquad\qquad (A2.3)$$

$$\begin{Bmatrix} a & b & s \\ c & d & u \end{Bmatrix} \, C(cds;\, \gamma\,\delta)\, C(abs;\, \alpha\beta),$$

where $C(cbu;\, \gamma\,{-}\beta) \equiv \langle c,\gamma;\, b,{-}\beta \,|c,b;u,\gamma-\beta\rangle$ is the vector-coupling
coefficient and $\begin{Bmatrix} a & b & s \\ c & d & u \end{Bmatrix}$ is a 6 - j symbol. The solution for $M^s(s')$
is

$$M^s(s') \;=\; \sum_{u'} \, X_{s'u'} \; M^u(u') , \qquad\qquad (A2.4)$$

$$X_{su} \;=\; \xi_{su}(-1)^{b+d+\alpha+\gamma}\, (2u+1)\, \begin{Bmatrix} a & b & s \\ c & d & u \end{Bmatrix} , \qquad (A2.5)$$

and X_{su} is the crossing matrix.

We return to Eq. (A2.2) to evaluate ξ_{su} . Since we are crossing pseudoscalar mesons, we need consider only the π-, η-, and K-meson fields. The phase conventions are revealed in the field operators. The π field is

$$\phi_\pi^{(\mu)}(x) = \sum_{\underset{\sim}{k}} \left\{ f_{\underset{\sim}{k}}(x)\, a_\pi^{(\mu)}(\underline{k}) + (-1)^\mu\, f_{\underset{\sim}{k}}^*(x)\, a_\pi^{(-\mu)\dagger}(\underline{k}) \right\} , \quad (A2.6a)$$

where μ is the third component of isospin, and

$$f_{\underset{\sim}{k}}(x) = (2\, \omega_{\underset{\sim}{k}}\, V)^{-\frac{1}{2}}\, e^{-ik\cdot x} .$$

To solve for $a_\pi^{(\mu)}(\underset{\sim}{k})$ and $a_\pi^{(\mu)\dagger}(\underset{\sim}{k})$, we need the orthogonality relations,

$$\int d^3\underset{\sim}{x}\, f_{\underset{\sim}{k}'}^*(x)\, i\overset{\leftrightarrow}{\partial}_0\, f_{\underset{\sim}{k}}(x) = \delta^3(\underset{\sim}{k}' - \underset{\sim}{k}) , \quad (A2.7a)$$

$$\int d^3x\, f_{\underset{\sim}{k}}(x)\, i\overset{\leftrightarrow}{\partial}_0\, f_{\underset{\sim}{k}}(x) = 0 . \quad (A2.7b)$$

Combining Eqs. (A2.7) and (A2.6a), we find

$$a_\pi^{(\mu)}(\underset{\sim}{k}) = \int d^3x\, f_{\underset{\sim}{k}}^*(x)\, i\overset{\leftrightarrow}{\partial}_0\, \phi_\pi^{(\mu)}(x) , \quad (A2.6b)$$

$$a_\pi^{(\mu)\dagger}(\underset{\sim}{k}) = (-1)^\mu \int d^3x\, \phi_\pi^{(-\mu)}\, i\partial_0\, f_{\underset{\sim}{k}}(x) . \quad (A2.6c)$$

The η field is obtained by replacing π with η in Eq. (A2.6), setting $\mu = 0$, then dropping the index, μ .

The K and $\bar{K}$ mesons do not belong to the same isomultiplet, so the K-meson field is defined by

$$\psi_K^{(\mu)}(x) = \sum_{\underset{\sim}{k}} \left\{ f_{\underset{\sim}{k}}(x) \, a_K^{(\mu)}(\underset{\sim}{k}) + (-1)^{K+\mu} f_{\underset{\sim}{k}}^*(x) \, a_{\bar{K}}^{(-\mu)\dagger}(\underset{\sim}{k}) \right\}, \quad (A2.8a)$$

where K is also the isospin of the K meson and μ is the third component. Inversion of the field operator gives,

$$a_K^{(\mu)}(\underset{\sim}{k}) = \int d^3x \, f_{\underset{\sim}{k}}^*(x) \, i \overleftrightarrow{\partial}_0 \, \psi_K^{(\mu)}(x) ,$$

$$a_{\bar{K}}^{(\mu)}(\underset{\sim}{k}) = (-1)^{-K+\mu} \int d^3x \, f_{\underset{\sim}{k}}^*(x) \, i \overleftrightarrow{\partial}_0 \, \psi_K^{(-\mu)\dagger} ,$$

$$(A2.8b)$$

$$a_K^{(\mu)\dagger}(\underset{\sim}{k}) = \int d^3x \, \psi^{(\mu)\dagger}(x) \, i \overleftrightarrow{\partial}_0 \, f_{\underset{\sim}{k}}(x) ,$$

$$a_{\bar{K}}^{(\mu)\dagger}(\underset{\sim}{k}) = (-1)^{-K+\mu} \int d^3x \, \psi_K^{(-\mu)}(x) \, i \overleftrightarrow{\partial}_0 \, f_{\underset{\sim}{k}}(x) .$$

A simple application of the L. S. Z. reduction formalism is sufficient for determining ξ_{su} . After reducing the initial and final mesons out of the s-channel S-matrix element, and out of the u-channel S-matrix element, we compare the two S-matrix elements. A crossing condition results, and comparison with Eq. (A2.2) gives ξ_{su} .

To see how this goes, consider the example where the s reaction is

$$\Sigma \, \pi \rightarrow N \, \overline{K} \; .$$

We retain the momentum labels, but ignore a possible unit operator for elastic scattering. Reducing the mesons out of the S-matrix element, we find

$$\langle N, \; \overline{K}(\underset{\sim}{k} \, \delta) \quad \text{out} \quad | \Sigma \; ; \; \pi(\underset{\sim}{k}'\beta) \; \text{in} \rangle$$

$$= \; \langle N \; \text{out} \; | a_{\overline{K}}^{(\delta)} (\underset{\sim}{k}) \; a_{\pi}^{(\beta)\dagger}(\underset{\sim}{k}') | \Sigma \; \text{in} \rangle$$

$$= \; (-1)^{-K+\delta} \, (-1)^{\beta} \; i^2 \int d^4x \, d^4y \; f_{\underset{\sim}{k}}^{\;*}(x) \; f_{\underset{\sim}{k}'}(y)$$

$$\times \; (\Box_x + m_K^{\;2}) \, (\Box_y + m_\pi^{\;2}) \; \langle N | T \left\{ \psi_K^{(-\delta)\dagger}(x) \; \phi_\pi^{(-\beta)}(y) \right\} | \Sigma \rangle \; .$$

A similar calculation for the u reaction,

$$\Sigma \, K \; \rightarrow \; N \, \overline{\pi} \; ,$$

yields

$$\langle N \; ; \; \pi(\underset{\sim}{q}, -\beta) \; \text{out} \quad | \; \Sigma \; ; \; K(\underset{\sim}{q}', \, - \, \delta) \; \text{in} \rangle$$

$$= \; \langle N \; \text{out} \; | \; a_{\pi}^{(-\beta)} (\underset{\sim}{q}) \; a_K^{(-\delta)\dagger} (\underset{\sim}{q}') \; | \; \Sigma \; \text{in} \rangle$$

$$= \; i^2 \int d^4x \, d^4y \; f_{\underset{\sim}{q}}^{\;*}(y) \; f_{\underset{\sim}{q}'}(x)$$

(Equation continued)

$$\times (\Box_x + m_K{}^2)(\Box_y + m_\pi{}^2) \langle N|T \left\{ \phi_\pi{}^{(-\beta)}(y) \ \psi_K{}^{(-\delta)\dagger}(x) \right\} |\Sigma\rangle .$$

A comparison of these two expressions gives the crossing relation

$$S\left[\Sigma, \ \pi(\underset{\sim}{k}'\beta) \to N \ \overline{K}(\underset{\sim}{k} \ \delta)\right] = (-1)^{K-\delta-\beta} S[\Sigma, K(-\underset{\sim}{k}, -\delta) \to N, \ \pi(-\underset{\sim}{k}', -\beta)] .$$

The phase factor, ξ_{su} , is

$$(-1)^{K-\delta-\beta} .$$

This type of calculation is easily performed for the sixteen possibilities of incoming and outgoing π , η , K, or $\overline{K}$ mesons. The results are tabulated in Table A2.1.

From Table A2.1, it is clear that X_{su} is just a phase times $(2u + 1) \begin{Bmatrix} a & b & s \\ c & d & u \end{Bmatrix}$. The derivation of the isospin crossing matrices is now reduced to looking up $6-j$ symbols. The crossing matrices are found in Table A2.2. In this phase convention, the S matrix is symmetric (see Carruthers and Krisch[11]). The couplings derived in Appendix I and Table A2.2 imply the matrices, N_0 , shown in Table 2.1. Perhaps we should note that there are some phase differences between our N_0 and those calculated by Martin and Wali.[6]

TABLE A2.1: The Phase Factor, ξ_{su} , for Eqs. (A2.2) and (A2.5).

Mesons in s channel		ξ_{su}	$\xi_{su}(-1)^{d+b+\gamma+\alpha}$
Incoming b	Outgoing d		
π	π		
π	η	$(-1)^{\delta-\beta}$	$(-1)^{2a+b+d}$
η	π		
η	η		
K	K	$(-1)^{b+d+\beta+\delta}$	$(-1)^{2b+2c}$
K	$\overline{K}$	$(-1)^{b+d+\beta-\delta}$	$(-1)^{2a}$
$\overline{K}$	K	$(-1)^{b+d+\delta-\beta}$	$(-1)^{2c}$
$\overline{K}$	$\overline{K}$	$(-1)^{b+d-\beta-\delta}$	$(-1)^{2d+2c}$
π,η	K	$(-1)^{d+\delta-\beta}$	$(-1)^{2c+b}$
π,η	$\overline{K}$	$(-1)^{d-\delta-\beta}$	$(-1)^{2a+b}$
K	π,η	$(-1)^{b+\beta+\delta}$	$(-1)^{2a+d}$
$\overline{K}$	π,η	$(-1)^{b-\beta+\delta}$	$(-1)^{2c+d}$

TABLE A2.2: Isospin Crossing Matrices, X_{su}, For Baryon-Meson Scattering.

The symbols (s') and [u'] denote $M^s(s')$ and $M^u(u')$, respectively. The baryon exchanges needed in Section II are listed in the final two columns.

Channel	$\xi_{su}(-1)^{b+d+\gamma+\alpha}$	$M^s(s')$	$X_{s'u'}$		$M^u(u')$	Baryon Exchange	
						s-channel isospin	Baryon exchanged
$N\pi \to N\pi$	-	(1/2)	$-1/3$	$4/3$	[1/2]	3/2	N
		(3/2)	$2/3$	$1/3$	[3/2]		
$N\pi \to \Sigma K$	-	(1/2)	$-1/\sqrt{6}$	1	[0]	3/2	Λ, Σ
		(3/2)	$1/\sqrt{6}$	$1/2$	[1]		
$\Sigma K \to \Sigma K$	-	(1/2)	$-1/3$	$4/3$	[1/2]	3/2	Ξ
		(3/2)	$2/3$	$1/3$	[3/2]		
$N\bar{K} \to N\bar{K}$	+	(0)	$-1/2$	$3/2$	[0]		
		(1)	$1/2$	$1/2$	[1]	1	None
$N\bar{K} \to \Sigma\pi$	-	(0)	$-2/\sqrt{6}$	$4/\sqrt{6}$	[1/2]		
		(1)	$2/3$	$2/3$	[3/2]	1	N
$N\bar{K} \to \Lambda\pi$	-	(1)	$-2/\sqrt{6}$		[1/2]	1	N

(Table A2.2 continued)

Channel	$\xi_{su}(-1)^{b+d+\gamma+\alpha}$	$M^s(s')$	$X_{s'u'}$	$M^u(u')$	Baryon Exchange s-channel isospin	Baryon exchanged
$N\bar{K} \to \Xi K$	−	(0)	$\begin{pmatrix} 1/2 & -3/2 \\ -1/2 & -1/2 \end{pmatrix}$	[0]	1	Λ, Σ
		(1)		[1]		
$N\bar{K} \to \Sigma\eta$	+	(1)	$2/\sqrt{6}$	[1/2]	1	N
$\Sigma\pi \to \Sigma\pi$	+	(0)	$\begin{pmatrix} 1/3 & -1 & 5/3 \\ -1/3 & 1/2 & 5/6 \\ 1/3 & 1/2 & 1/6 \end{pmatrix}$	[0]		
		(1)		[1]	1	Λ, Σ
		(2)		[2]		
$\Sigma\pi \to \Lambda\pi$	+	(1)	-1	[1]	1	Σ
$\Sigma\pi \to \Xi K$	+	(0)	$\begin{pmatrix} 2/\sqrt{6} & -4/\sqrt{6} \\ -2/3 & -2/3 \end{pmatrix}$	[1/2]	1	Ξ
		(1)		[3/2]		
$\Sigma\pi \to \Sigma\eta$	−	(1)	1	[1]	1	Σ
$\Lambda\pi \to \Lambda\pi$	+	(1)	1	[1]	1	Σ
$\Lambda\pi \to \Xi K$	+	(1)	$2/\sqrt{6}$	[1/2]	1	Ξ
$\Lambda\pi \to \Sigma\eta$	−	(1)	$-1/\sqrt{3}$	[0]	1	Λ

(Table A2.2 continued)

Channel	$\xi_{su}(-1)^{b+d+\gamma+\alpha}$	$M^s(s')$	$X_{s'u'}$		$M^u(u')$	Baryon Exchange	
						s-channel isospin	Baryon exchanged
$\Xi K \to \Xi K$	$+$	(0)	$-1/2$	$3/2$	$[0]$	1	None
		(1)	$1/2$	$1/2$	$[1]$		
$\Xi K \to \Sigma\eta$	$-$	(1)	$-2/\sqrt{6}$		$[1/2]$	1	Ξ
$\Sigma\eta \to \Sigma\eta$	$+$	(1)	1		$[1]$	1	Σ
$\Xi\pi \to \Xi\pi$	$-$	$(1/2)$	$-1/3$	$4/3$	$[1/2]$	$1/2$	Ξ
		$(3/2)$	$2/3$	$1/3$	$[3/2]$		
$\Xi\pi \to \Lambda\bar{K}$	$+$	$(1/2)$	$3/\sqrt{6}$		$[1]$	$1/2$	Σ
$\Xi\pi \to \Sigma\bar{K}$	$+$	$(1/2)$	$1/\sqrt{6}$	-1	$[0]$	$1/2$	Λ,Σ
		$(3/2)$	$-1/\sqrt{6}$	$-1/2$	$[1]$		
$\Xi\pi \to \Xi\eta$	$+$	$(1/2)$	1		$[1/2]$	$1/2$	Ξ
$\Lambda\bar{K} \to \Lambda\bar{K}$	$-$	$(1/2)$	1		$[1/2]$	$1/2$	N
$\Lambda\bar{K} \to \Sigma\bar{K}$	$-$	$(1/2)$	-1		$[1/2]$	$1/2$	N
$\Lambda\bar{K} \to \Xi\eta$	$-$	$(1/2)$	$1/\sqrt{2}$		$[0]$	$1/2$	Λ
$\Sigma\bar{K} \to \Sigma\bar{K}$	$-$	$(1/2)$	$-1/3$	$4/3$	$[1/2]$	$1/2$	N
		$(3/2)$	$2/3$	$1/3$	$[3/2]$		
$\Sigma\bar{K} \to \Xi\eta$	$-$	$(1/2)$	$-3/\sqrt{6}$		$[1]$	$1/2$	Σ
$\Xi\eta \to \Xi\eta$	$-$	$(1/2)$	1		$[1/2]$	$1/2$	Ξ
$\Xi\bar{K} \to \Xi\bar{K}$	$+$	(0)	$-1/2$	$3/2$	$[0]$	0	Λ,Σ
		(1)	$1/2$	$1/2$	$[1]$		

APPENDIX III: SOME INTEGRALS

The integrals needed in the calculations of Section III and the mass expansions of Section IV were done analytically. We list here the results of these computations. The solution to the N/D equations in Section III was reduced to evaluating the integral,

$$E(s; M, \mu) = \frac{s - t}{\pi} \text{ P.V.} \int_\beta^\infty dx \frac{[k(x)]^{3/2}}{x^2 (x - t)^2 (x - s)} , \qquad \text{(A3.1a)}$$

where

$$k(x) = x^2 - 2bx + c ,$$

$$b = (M^2 + \mu^2) ,$$

$$c = (M^2 - \mu^2)^2 ,$$

$$\beta = (M + \mu)^2 . \qquad \text{(A3.1b)}$$

A partial fraction decomposition $\left(\text{with } k^2(x) \text{ in the numerator}\right)$ and integration of each term yields

$$(s - t)^{-1} \pi E(s; M, \mu) = t^{-2} [cs^{-1} + k(t) (s - t)^{-1}] \qquad \text{(A3.2)}$$

$$+ c^{\frac{1}{2}} t^{-3} s^{-2} [c (t + 2s) - 3stb] \ln(\mu M^{-1}) + k^{\frac{1}{2}}(t) t^{-3} (t - s)^{-2}$$

$$\times [t^2(s - 3b) + (3c + sb) t - 2sc] L(t) - k^2(s) s^{-2} (s - t)^{-2} X(s),$$

where

$$L(t) = \ell n \, \left| [b - t - k^{\frac{1}{2}}(t)]/2M\mu \right| ,$$

and

$$X(s) = k^{-\frac{1}{2}}(s) \, \ell n \, \left| [b - s - k^{\frac{1}{2}}(s)]/(2M\,\mu) \right|, k(s) > 0$$

$$(A3.3)$$

$$X(s) = -[-k(s)]^{-\frac{1}{2}} \, \{ \tan^{-1} [(s - b)/(-k(s))^{\frac{1}{2}}] + \pi/2 \}, k(s) < 0 .$$

The apparent singularity at $s = (M - \mu)^2$ has zero discontinuity. Thus, the two forms of $X(s)$ in Eq. (A3.3) are simple analytic continuations of one another.

To second order in the mass symmetry breaking, the "mass expansion" of $E(s;M,\mu)$ is

$$E(s;M,\mu) = E(s;M_0 , \mu_0) + E_1(s) + E_2(s) , \qquad (A3.4)$$

where

$$E_1(s) = \frac{\partial}{\partial(M^2)} \, E(s;M,\mu) \Big|_{M_0^2, \mu_0^2} \Delta + \frac{\partial}{\partial(\mu^2)} \, E(s;M,\mu) \Big|_{\mu_0^2, \mu_0^2} \delta ,$$

$$E_2(s) = \frac{1}{2} \, \frac{\partial^2}{\partial(M^2)^2} \, E(s;M,\mu) \Big|_{M_0^2, \mu_0^2} \Delta^2 + \frac{\partial^2}{\partial(M^2)\partial(\mu^2)} \, E(s;M,\mu) \Big|_{M_0^2, \mu_0^2} \Delta\delta$$

$$+ \frac{1}{2} \, \frac{\partial^2}{\partial(\mu^2)^2} \, E(s;M,\mu) \Big|_{M_0^2, \mu_0^2} \delta^2 ,$$

and

$$\Delta = (M^2 - M_0{}^2) ,$$

$$\delta = (\mu^2 - \mu_0{}^2) .$$

Since the integrand of $E(s;M,\mu)$ is uniformly continuous for all s, we can differentiate $E(s;M,\mu)$ under the integral sign,

$$E_1(s;M,\mu) = \frac{3}{\pi} (s - t) \; \text{P.V.} \int_{\beta_0}^{\infty} dx \; \frac{k^{\frac{1}{2}}(x) \; (d - ex)}{x^2 (x - t)^2 (x - s)} \qquad (A3.5)$$

with

$$d = (M_0{}^2 - \mu_0{}^2) (\Delta - \delta) ,$$

$$e = \Delta + \delta .$$

Another partial fraction decomposition and integration gives

$$3^{-1}(s - t)^{-1} \pi E_1(s) = t^{-2} [ds^{-1} - (d - et) (t - s)^{-1}]$$

$$+ s^{-2} t^{-3} c^{-\frac{1}{2}} [cd(t + 2s) - st(ce + bd)] \; \ell n(\mu_0 M_0{}^{-1})$$

$$- k^{-\frac{1}{2}}(t) t^{-3} (t - s)^{-2} \{t(t - s) (d - et) (t - b)$$

$$- k(t) [d(3t - 2s) + et (s - 2t)]\} \; L(t)$$

$$- k(s) s^{-2}(s - t)^{-2} (d - es) \; X(s) . \qquad (A3.6)$$

If $s \neq \beta_0$, we can take a second mass derivative of $E(s; M, \mu)$,

$$E_2(s) = \frac{3}{\pi} (s - t) \; \text{P.V.} \int_{\beta_0}^{\infty} dx \; \frac{k^{-\frac{1}{2}}(x) \, [f \, x^2 + g \, x + h]}{x^2 (x - t)^2 (x - s)} , \quad (A3.7)$$

where

$$f = \Delta^2 + \delta^2$$

$$g = -2 (M_0^2 \, \Delta + \mu_0^2 \, \delta) (\Delta^2 - \delta^2) ,$$

$$h = (M_0^2 - \mu_0^2)^2 (\Delta - \delta)^2 .$$

The integral, Eq. (A3.7), is then

$$3^{-1} (s - t)^{-1} \pi \, E_2(s) = s^{-1} c^{-1} t^{-2} h - (f \, t^2 + g \, t + h) \, /$$

$$[t^2 (t - s) \, k(t)] + [c^{-3/2} \, t^{-2} \, s^{-1} \, b \, h$$

$$+ t^{-3} \, s^{-2} \, c^{-1/2} \, (s \, t \, g + h \, t + 2 \, h \, s)] \, \ln (\mu_0 \, M_0^{-1})$$

$$- k^{-\frac{1}{2}} (t) \, \{ (f \, t^2 + g \, t + h) (b - t) \, t^{-2} \, (t - s)^{-1} \, k^{-1}(t)$$

$$+ t^{-3} \, (t - s)^{-2} \, [t(t - s) \, (2 \, f \, t + g) - (f \, t^2 + g \, t + h) \quad (A3.8)$$

$$\times (3t - 2s)] \} \, L(t) - s^{-2} (s - t)^{-2} \, (f \, s^2 + g \, s + h) \, X(s) .$$

Equation (A3.8) is infinite at $s = \beta_0$. However, for s near β_0, the integrand of $E_1(s)$ is no longer uniformly continuous, and we must separate the integral into two parts in order to decide how $E_2(s)$ behaves at $s = \beta_0$. We write

$$E_1(s;M,\mu) = \frac{3}{\pi}(s-t) \text{ P.V.} \int_{\beta_0}^{\infty} dx \, \frac{(x-\beta_0)^{\frac{1}{2}}}{x(x-s)} \{\alpha(x;M_0,\mu_0) - \alpha(\beta_0;M_0,\mu_0)\}$$

$$+ \frac{3}{\pi}(s-t)\,\alpha(\beta_0;M_0\mu_0) \text{ P.V.} \int_{\beta_0}^{\infty} dx \, \frac{(x-\beta_0)^{\frac{1}{2}}}{x(x-s)}, \quad (A3.9)$$

where

$$\alpha(x;M,\mu) = x^{-1}(x-t)^{-2}(d-ex)[x-(M-\mu)^2]^{\frac{1}{2}}.$$

The integrand in the first integral of Eq. (A3.9) is uniformly continuous for all s and the mass derivatives exist. The second integral can be done explicitly, and then differentiated.

$$\text{P.V.} \int_{\beta}^{\infty} dx \, \frac{(x-\beta)^{\frac{1}{2}}}{x(x-s)} = \frac{\pi}{2}\beta^{\frac{1}{2}}, \qquad s \geqslant \beta$$

$$= \frac{\pi}{2}[\beta^{\frac{1}{2}} - (\beta-s)^{\frac{1}{2}}], \; s < \beta.$$

When $(\beta-s)^{\frac{1}{2}}$ is differentiated, there is a $(\beta-s)^{-\frac{1}{2}}$ singularity at $s = \beta$. Thus, spurious zeros are introduced into $\det[D(s)]$ in the second order mass expansion. The mass expansion is not very reliable when the dynamically-produced zero in $\det[D(s)]$ lies close to $s = \beta_0$.

FOOTNOTES AND REFERENCES

1. M. Gell-Mann, _Proceedings of the International Conference on High-Energy Nuclear Physics, Geneva, 1962_ (CERN Scientific Information Service, Geneva, Switzerland, 1962). S. L. Glashow and J. J. Sakari, Nuovo Cimento $\underline{25}$, 337 (1962), also predicted the Ω^- if the $N_{3/2}^*$ (1236) and Y_1^* (1385) belongs to a decuplet representation. But they felt then that it was more likely that these particles belong to a 27-plet representation.

2. See M. Gell-Mann and Y. Ne'eman, The _Eightfold Way_ (W. A. Benjamin and Co., New York, 1965), p. 85, for a brief review of this history.

3. V. E. Barnes, P. L. Connolly, D. J. Crennell, et al., Phys. Rev. Letters, $\underline{12}$, 204 (1964).

4. R. F. Dashen and S. C. Frautschi, Phys. Rev. $\underline{137}$, B1331 (1965). Further references may be found in this paper.

5. G. F. Chew, _The Analytic S Matrix_ (W. A. Benjamin and Co., New York, 1966).

6. A. W. Martin and K. C. Wali, Phys. Rev. $\underline{130}$, 2455 (1963).

7. F. J. Ernst, R. L. Warnock, and K. C. Wali, Phys. Rev. $\underline{141}$, 1354 (1966).

8. R. F. Dashen and S. C. Frautschi, Phys. Rev. $\underline{137}$, B1318 (1965).

9. K. C. Wali and R. L. Warnock, Phys. Rev. $\underline{135}$, B1358 (1964).

10. S. L. Glashow and M. Muraskin, Phys. Rev. $\underline{132}$, 482 (1963).

11. P. A. Carruthers and J. P. Krisch, Ann. Phys. $\underline{33}$, 1 (1965).

12. J. J. DeSwart, Rev. Mod. Phys. $\underline{35}$, 916 (1963).

13. S. Mandelstam, J. E. Paton, R. F. Peierls, et al., Ann. Phys. $\underline{18}$, 198 (1962).

PART B

EXACT EQUATIONS FOR THE PERTURBED AMPLITUDE AND MASS
AND COUPLING SHIFTS IN DISPERSION THEORY[*]

I. INTRODUCTION

A systematic assault on the total bootstrap problem seems
impossible at present. However, approximations based on the concept
of supermultiplets of strongly interacting particles reduce the
problem into more manageable units. After rough calculations have
been performed with the supermultiplets, it is possible to induce
symmetry breaking within the multiplet to obtain finer details.[1-3]
Computations are not too difficult if the symmetry breaking is treated
in a first-order S-matrix perturbation theory.[2] The usefulness of the
linearized theory is well demonstrated in the theory of octet enhancement.[3]

The perturbation consists of variations of the left- and right-
hand singularities of the partial-wave amplitude. The Dashen-Frautschi
theory[2] describes the mass and coupling shifts of a dynamically bound
state as a linear function of these variations. The linear theory is
capable of calculating small shifts when the bound-state pole remains
on a given Riemann sheet of the scattering amplitude. However, if the
pole changes sheets, or if it executes a large motion on a single
sheet, the linear theory is not adequate. For these and for mathemati-
cal reasons it is desirable to have a more complete theory of perturbed
amplitudes and of mass and coupling shifts of bound states.

Equations for the perturbed amplitude, and for the mass and

coupling shifts, have been derived by M. Kugler for single-channel potential theory[4] where only the left-hand singularities are varied. Using a Castillejo-Dalitz-Dyson (CDD) pole in his perturbed-amplitude equations, Kugler[4] then recovers the potential-theory analog of the Dashen-Frautschi mass-shift formula. The inclusion of many channels in his formalism is trivial. However, the generalization to the relativistic case in which the unitarity cuts are also varied is less simple.

In Section II, we propose a set of exact nonsingular equations for the perturbed amplitude. The input into these equations is the unperturbed amplitude in the form ND^{-1} and a perturbation represented by variations of the exchange and unitarity cuts. It is clear that this is sufficient information to calculate the total amplitude. Moreover, in a two-body elastic-unitary formalism, it is consistent with the bootstrap philosophy to use the change of the unitarity cuts as input, since without three-body intermediate states it is impossible to determine whether an external particle is a bound state or "elementary." At the end of Section II we show that the perturbed amplitude equations can account for the appearance of a stable-particle pole on the physical sheet, when the perturbation supplies the necessary additional binding force.

In Section III we find the mass shifts and the coupling-constant perturbations of a bound state when the unperturbed amplitude already has a pole on the same sheet. These are given in terms of the solutions to the equations derived in Section II. To describe the mass shift of a bound state, we note that the unperturbed and total amplitudes must each have simple pole, but located at different values of s . Thus, the perturbed amplitude must have <u>two</u> poles: one to

cancel the pole in the unperturbed amplitude and the other to correspond
to the bound state of the total amplitude. It is possible to achieve
this effect mathematically by reinterpreting the dynamical bound
state of the unperturbed amplitude as an elementary particle for the
calculation of the perturbed ampltiude.

The most obvious application of the mass- and coupling-shift
formulas of Section III is a perturbation expansion for these
quantities. In Section IV, which is divided into three subsections,
we derive formulas for the first-order mass shift, the first-order
coupling shift, and the second-order mass shift. The first-order
results are identical to those of Dashen and Frautschi.[2] The second-
order coupling shifts and higher order terms in the perturbation
expansions are easy to derive, but the complicated results are
probably of little use in numerical calculations.

II. EQUATIONS FOR THE PERTURBED AMPLITUDE

Suppose the many-channel partial-wave scattering amplitude, $A(s)$, can be written as a sum of two terms,

$$A(s) = A_0(s) + A_1(s) , \qquad (2.1)$$

where we shall call $A_0(s)$ the "unperturbed amplitude" and $A_1(s)$ the "perturbed amplitude." Restricting ourselves to two-body channels and two-body unitarity, we assume that A_0 is known in the form

$$A_0(s) = N(s) D^{-1}(s) . \qquad (2.2)$$

The discontinuity relations for $N(s)$ and $D(s)$ are the usual ones: $D(s)$ has only a right-hand cut,

$$[D(s)]_R \equiv (2i)^{-1} [D(s + i\epsilon) - D(s - i\epsilon)] = - \rho_0(s) N(s): \qquad (2.3a)$$

and $N(s)$ has only left-hand singularities,

$$[N(s)]_L \equiv (2i)^{-1} [N(s - i\epsilon) - N(s + i\epsilon)] = V_0(s) D(s) . \qquad (2.3b)$$

Moreover, $A(s)$, $A_0(s)$, and $A_1(s)$ are symmetric and Hermitian analytic.

The input for the calculation of the perturbed amplitude is the change of the unitarity cuts,

$$\delta\rho(s) = \rho(s) - \rho_0(s) , \qquad (2.4a)$$

where

$$[A(s)]_R = A^\dagger(s) \rho(s) A(s) , \qquad (2.4b)$$

and the change of the left-hand singularities,

$$V'(s) = V(s) - V_0(s) , \qquad (2.4c)$$

with

$$[A(s)]_L = V(s) . \qquad (2.4d)$$

Neither $V'(s)$ nor $\delta\rho(s)$ is assumed to be small in this section.

To derive equations for $A_1(s)$, it is convenient to define[2]

$$J(s) = \widetilde{D}(s) A_1(s) D(s) . \qquad (2.5)$$

The tilde signifies matrix transpose. Since $J(s)$ has separate left and right singularities, it can be factored into the form

$$J(s) = n(s) d^{-1}(s) . \qquad (2.6)$$

The discontinuity relation for $J(s)$ is sufficiently complicated that if all the right cuts are put into $d(s)$ and all the left cuts are put into $n(s)$, then the equations for $n(s)$ and $d(s)$ are nonlinear. To preserve the linearity of the equations, $n(s)$ must contain some of the right cuts. The equations for $n(s)$ and $d(s)$ are then singular, but they are very similar to the three-body

ND^{-1} equations derived by Mandelstam.[5] By following Mandelstam's analysis, we use the standard techniques[6] for reducing the Cauchy-singular equations to nonsingular equations.

The discontinuity of $A_1(s)$ on the right is needed for deriving the discontinuity relation for $J(s)$. From Eqs. (2.1), (2.3), and (2.4), we find

$$[A_1]_R = A_0{}^\dagger \, \delta\rho \, A_0 + A_0{}^\dagger \rho \, A_1 + A_1{}^\dagger \rho \, A_0 + A_1{}^\dagger \rho \, A_1 . \tag{2.7}$$

In transforming Eq. (2.7) into a discontinuity relation for $J(s)$, we use the fact that J is hermitian analytic,[7]

$$J^\dagger = J^{(-)} . \tag{2.8}$$

Substitute Eqs. (2.5) and (2.8) into Eq. (2.7), multiply on the left by $D^\dagger$ and on the right by D, then use the relation,

$$D^{-1} D^* = I + 2iD^{-1} \rho_0 N. \tag{2.9}$$

The discontinuity of J across the right cuts is then

$$[J]_R = J^\dagger G J + J^\dagger B^\ddagger + BJ + T , \tag{2.10a}$$

where

$$\begin{aligned} G &= \widetilde{D}^{-1\dagger} \rho \, \widetilde{D}^{-1} , \\ B &= N^\dagger \, \delta\rho \, \widetilde{D}^{-1} , \\ T &= N^\dagger \, \delta\rho \, N . \end{aligned} \tag{2.10b}$$

The discontinuity of J across the left cuts follows from Eq. (2.4),

$$[J]_L = L \equiv \widetilde{D} V' D .\tag{2.10c}$$

To obtain linear equations for n and d in Eq. (2.6), the last two terms of Eq. (2.10a) are put into the discontinuity of n. The coupled equations for n and d are

$$d(s) = I - \frac{1}{\pi} \int_R ds' \frac{G(s') \, n(s')}{s' - s - i\epsilon} - \frac{1}{\pi} \int_R ds' \frac{B^\dagger(s') \, d(s')}{s' - s - i\epsilon} ,\tag{2.11a}$$

$$n(s) = \frac{1}{\pi} \int_L ds' \frac{L(s') \, d(s')}{s' - s + i\epsilon} + \frac{1}{\pi} \int_R ds' \frac{T(s') \, d(s')}{s' - s - i\epsilon}$$

$$+ \frac{1}{\pi} \int_R ds' \frac{B(s') \, n(s')}{s' - s - i\epsilon} .\tag{2.11b}$$

The exact limits of integration are obvious from the discontinuity relations, Eq. (2.10).

Equations (2.11a) and (2.11b) are both Cauchy singular. The reader who is uninterested in the technical details of finding equivalent nonsingular equations should now turn to the text below Eq. (2.19b). Equations (2.11a) and (2.11b) are conveniently reduced to nonsingular equations if we first remove the d term from the right-hand side of Eq. (2.11a) and the n term from the right-hand side of Eq. (2.11b). This can be done by defining

$$d(s) = m(s) f(s) ,\tag{2.12a}$$

$$n(s) = t(s) u(s) ,\tag{2.12b}$$

where $m(s)$ and $t(s)$ satisfy the equations,

$$m(s) = I - \frac{1}{\pi} \int_R ds' \frac{B^\dagger(s') m(s')}{s' - s - i\epsilon} ,\tag{2.13a}$$

$$t(s) = I + \frac{1}{\pi} \int_R ds' \frac{B(s) t(s')}{s' - s - i\epsilon} .\tag{2.13b}$$

Equations (2.13a,b) are Cauchy singular, but are easily reduced to nonsingular equations. (We do this later). To find equations for f and u, compare the discontinuities of Eq. (2.12) and (2.11). The formula for finding the discontinuity in f is

$$[mf]_R = m^{(-)} [f]_R + [m]_R f .\tag{2.14}$$

The integral representation of f (or u) is easily constructed. The equations for f and u in matrix form are

$$\begin{pmatrix} f(s) \\ u(s) \end{pmatrix} = \begin{pmatrix} I \\ \frac{1}{\pi} \int_L ds' \frac{\lambda(s') f(s')}{s' - s + i\epsilon} \end{pmatrix} + \frac{1}{\pi} \int_R \frac{ds'}{s' - s - i\epsilon}$$

$$\times \begin{pmatrix} 0 & -\gamma(s') \\ \tau(s') & 0 \end{pmatrix} \begin{pmatrix} f(s') \\ u(s') \end{pmatrix} ,\tag{2.15a}$$

where

$$\lambda(s) = [t^{(-)}(s)]^{-1} L(s) m(s) ,$$

$$r(s) = [m^{(-)}(s)]^{-1} G(s) t(s) , \qquad (2.15b)$$

$$\tau(s) = [t^{(-)}(s)]^{-1} T(s) m(s) .$$

All four equations for m, t, f, and u are Cauchy singular. Equation (2.13a) is reduced to a nonsingular equation by operating on both sides of the equation from the left with[5]

$$I - \frac{1}{\pi} \int_R ds' \frac{B^\dagger(s')}{s' - s + i\epsilon} .$$

The nonsingular equation for $m(s)$ is

$$m(s) = I - [I + 2i B^\dagger(s)]^{-1} \left\{ b(s) \right.$$

$$+ \frac{1}{\pi} \int_R ds' \frac{b^{(-)}(s') - b^{(-)}(s)}{s' - s} B^\dagger(s') m(s') \left. \right\} , \qquad (2.16a)$$

where

$$b(s) = \frac{1}{\pi} \int_R ds' \frac{B^\dagger(s')}{s' - s - i\epsilon} . \qquad (2.16b)$$

The operator for reducing Eq. (2.13b) is

$$I + \frac{1}{\pi} \int_R ds' \frac{B(s')}{s' - s + i\epsilon} .$$

The nonsingular equation for $t(s)$ is

$$t(s) = I + [I - 2i\ B(s)]^{-1} \left\{ b_1(s) \right.$$

$$\left. - \frac{1}{\pi} \int_R ds' \frac{b_1^{(-)}(s') - b_1^{(-)}(s)}{s' - s} B(s')\ t(s') \right\},$$

(2.17a)

where

$$b_1(s) = \frac{1}{\pi} \int_R ds' \frac{B(s')}{s' - s - i\epsilon} .$$

(2.17b)

The reduction of the coupled equations for f and u is facilitated by the matrix notation in Eq. (2.13c). Operate on both sides of the equation from the left with

$$I + \frac{1}{\pi} \int_R \frac{ds'}{s' - s + i\epsilon} \begin{pmatrix} 0 & -\gamma(s') \\ \tau(s') & 0 \end{pmatrix} .$$

The reduced equations are

$$f(s) - I + 2i\ \gamma(s)\ u(s) = \frac{1}{\pi} \int_R ds' \frac{r_I^{(-)}(s') - r_I^{(-)}(s)}{s' - s} \tau(s')\ f(s')$$

$$+ \frac{1}{\pi} \int_L ds' \frac{r_I^{(-)}(s') - r_I^{(-)}(s)}{s' - s} \lambda(s')\ f(s') , \quad (2.18a)$$

$$r_I(s) = \frac{1}{\pi} \int_R ds' \frac{r(s')}{s' - s - i\epsilon} , \qquad (2.18b)$$

$$u(s) - 2i\,\tau(s)\,[f(s) - I] = \frac{1}{\pi} \int_L \frac{ds'}{s' - s + i\epsilon}\,\lambda(s')\,f(s')$$

$$+ \tau_I(s) + \frac{1}{\pi} \int_R ds' \frac{\tau_I^{(-)}(s') - \tau_I^{(-)}(s)}{s' - s}\,\gamma(s')\,u(s') , \quad (2.19a)$$

$$\tau_I(s) = \frac{1}{\pi} \int_R \frac{ds'}{s' - s - i\epsilon}\,\tau(s') . \qquad (2.19b)$$

Our final set of Cauchy-singularity-free equations for the perturbed amplitude is Eqs. (2.16) through (2.19). The integrals of Eqs. (2.18) and (2.19) are linear in the perturbation, and the kernels of Eqs. (2.16) and (2.17) are already of second order. Thus, simply expanding n and d in a Neumann series will lead to a $J(s)$ which is the ratio of two power series in a parameter describing the perturbation. It is then possible for $J(s)$ to develop poles as the perturbation is changed. Even in a first-order iteration of d, this gives a mechanism for describing the binding of a resonance into a stable-particle pole, i.e., the appearance of a pole at threshold on the physical sheet. The emergence of resonance poles onto the unphysical sheet is described in the same way, but Eq. (2.11) must be continued onto the second sheet. (The details of a similar analytic continuation are found in Sec. III.)

Kugler[4] has studied in single-channel potential theory[8] the appearance of poles at threshold when the perturbation supplies the final binding force. With an effective range formula, he found

that the first iteration of f correctly described the motion of the pole as it moved away from threshold. In the next section, we assume the pole is already present in the unperturbed amplitude, and that the perturbation merely shifts the position of the pole on the same sheet.

III. MASS AND COUPLING-CONSTANT SHIFTS OF BOUND STATES

The ND^{-1} technique is frequently used in dynamical calcula-
tions to find the masses and coupling constants of the composite
particles communicating with a given set of channels and generated
by a certain set of input forces. The mass of the bound state
satisfies

$$\det [D(s_B)] = 0 . \qquad\qquad (3.1)$$

Since the equations of Sec. II are readily continued to the unphysical
sheet (see below), we use the term "bound state" to mean either a
stable particle or a resonance pole. However, we now restrict the
perturbation so that the pole will remain on the same sheet. The
case in which the pole does change sheets was briefly discussed at
the end of the preceding section.

We now derive exact mass- and coupling-shift formulas. Let
Eq. (3.1) have only one physical solution. Since the pole in A
is shifted with respect to the pole in A_0 , the amplitude A_1 must
have two poles: one to cancel the pole in A_0 and the other to
represent the particle in the total amplitude. From Eqs. (2.5) and
(3.1), it is clear that the pole in A_0 can be cancelled only if

$$\det [J(s_B)] = 0 \qquad\qquad (3.2)$$

is a simple zero. Since $\det [D(s)]$ also has a simple zero at
s_B , $A_1(s)$ will have a simple pole at $s = s_B$.

Formally, we can satisfy Eq. (3.2) by utilizing the CDD
ambiguity in the $n\,d^{-1}$ equations of Section II. A CDD pole
is inserted into Eq. (2.11) to force the occurrence of a zero at
$s = s_B$. The $n\,d^{-1}$ equations for J are

$$d(s) = I - \frac{1}{\pi} \int_R ds' \frac{G(s')\,n(s')}{s' - s - i\epsilon} - \frac{1}{\pi} \int_R ds' \frac{B^\dagger(s')\,d(s')}{s' - s - i\epsilon}$$

$$- \frac{\Gamma}{s - s_B} , \qquad\qquad (3.3a)$$

$$n(s) = \frac{1}{\pi} \int_L ds' \frac{L(s')\,d(s')}{s' - s + i\epsilon} + \frac{1}{\pi} \int_R ds' \frac{T(s')\,d(s')}{s' - s - i\epsilon}$$

$$+ \frac{1}{\pi} \int_R ds' \frac{B(s')\,n(s')}{s' - s - i\epsilon} , \qquad\qquad (3.3b)$$

where $d(s)$ now satisfies an equation with one CDD pole. The residue
of the CDD pole is denoted by Γ ; the remaining terms are defined
in Section II. A cancellation between the CDD pole and the remainder
of the right side of Eq. (3.3a) will cause a pole in $J(s)$. The
location of the new pole satisfies

$$\det\,[d(s_B')] = 0 . \qquad\qquad (3.4)$$

Thus, the zero imposed on $J(s)$ by the CDD pole can be used to
cancel the pole in A_0 , and the pole generated by the CDD pole at
s_B' in $A_1(s)$ represents the particle when $\delta\rho$ and V' are
nonzero. The restriction to one bound state in the unperturbed
amplitude is trivially overcome by inserting several CDD poles into
Eq. (3.3a).

The situation for shifts of resonance poles on the second

sheet is similar except that Eq. (3.3) must be analytically

continued far enough onto the second sheet that the resonance

region is exposed. The correct continuation consists of re-

drawing the contours denoted by R so that they go below s_B .

Then the position of the resonance pole in the unperturbed amplitude

is explicitly exposed, and the CDD pole can be inserted as in the

case of a stable bound state. The proof that this is the correct

continuation is somewhat complicated by the fact that some of the

right cuts begin at the unperturbed threshold and others begin at

the perturbed threshold. If $\delta\rho$ were zero, then this would

certainly be the correct continuation. However, when $\delta\rho \neq 0$,

it would appear that the s_B that solves Eq. (3.1) would not be

on the sheet specified by the deformed cuts. This Oakes-Yang[9]

type dilemma is resolved by noting that there exists a family

of poles on the sheets connected by the _perturbed_ threshold. Con-

sequently there _is_ a resonance pole in the resonance region of

the _perturbed_ amplitude. Locating the CDD at this point would then

have the same consequences as in the case of a stable bound state.

Thus Eq. (3.3) is correct for the resonance case, except that R

represents contours that go below s_B , rather than just along the

real axis.

It is clear that the CDD pole gives the proper mathematical

behavior. We now give a more physical interpretation of the CDD

pole. The existence and properties of the particle were calculated

in finding A_0 . In the unperturbed amplitude, the particle-pole represents a dynamical bound state. However, the particle will be "elementary" in any further calculation. In this sense, an elementary particle is one whose existence and quantum numbers are available for further computation. Thus, the purpose of the CDD pole is to reinterpret the composite particle of the unperturbed amplitude as input (i.e., an elementary particle) for the calculation of the perturbed amplitude.

We determine Γ from the form of $A_0(s)$ near $s = s_B$,

$$A_0(s) \approx (s - s_B)^{-1} R , \tag{3.5a}$$

where R is the factorizable matrix of unperturbed channel-bound-state coupling constants. Since there exists a pole in $A_1(s)$ that cancels the pole in A_0 , $A_1(s)$ is

$$A_1(s) \approx - (s - s_B)^{-1} R \tag{3.5b}$$

for $s \approx s_B$. It follows from Eqs. (3.3), (3.5), (2.5) and (2.6) that

$$\Gamma = N^{-1}(s_B) R \, \widetilde{N}^{-1}(s_B) \, n(s_B) . \tag{3.6}$$

The total amplitude has a simple pole at $s = s_B'$. Since $A_0(s)$ is assumed well-behaved at $s = s_B'$,

$$A_1(s) \approx (s - s_B')^{-1} R' , \tag{3.5c}$$

where R' is the new·coupling matrix.

In order to find a convenient formula for the mass shift, we

define

$$F(s) = I - \frac{1}{\pi} \int_R ds' \frac{G(s')\, n(s')}{s' - s - i\epsilon} \tag{3.7}$$

$$- \frac{1}{\pi} \int_R ds' \frac{B^+(s)\, d(s)}{s' - s - i\epsilon} .$$

$F(s)$ is not simply related to $d(s)$ in Eq. (3.3) since the solution to the nd^{-1} equations without CDD poles is not simply related to the solution of the equations with CDD poles. To evaluate $F(s)$, Eq. (3.3) must first be solved, then the solution inserted into the defining equation for $F(s)$.

Equation (3.4) is equivalent to

$$\det [\delta s_B - F^{-1}(s_B')\, \Gamma] = 0 , \tag{3.8}$$

where

$$\delta s_B = s_B' - s_B$$

is just the mass shift of the bound state. Equation (3.8) has the appearance of an eigenvalue equation except that $F^{-1}(s)$ is evaluated at the unknown value of $s = s_B'$. However, it is extremely convenient to analyze Eq. (3.8) formally as an eigenvalue equation. Then there are n values (n is the number of channels) of δs_B which solve Eq. (3.8). Thus, $n-1$ of these must be zero for δs_B to be unique. The derivation of this result relies on the pole-factorization theorem for the bound-state pole residues,

$$R_{ij} = - g_i\, g_j . \tag{3.9}$$

From the Laplace expansion of Eq. (3.8), it follows by induction that

$$\det(\delta s_B - F^{-1}(s_B')\, \Gamma) = (\delta s_B)^{n-1} [\delta s_B - \operatorname{tr}(F^{-1}(s_B')\, \Gamma)] . \tag{3.10}$$

We emphasize that no approximation has been made. Equation (3.10) follows directly from the factorizability of $F^{-1}(s_B')\ \Gamma$. Consequently,

$$\delta\ s_B\ =\ \text{tr}[F^{-1}(s_B')\ \Gamma]\ . \tag{3.11}$$

Equation (3.9) aids in writing another expression for $\delta\ s_B$,

$$\delta\ s_B\ =\ -\ \underline{g}^T\ \widetilde{N}^{-1}(s_B)\ n(s_B)\ F^{-1}(s_B')\ N^{-1}(s_B)\ \underline{g} \tag{3.12}$$

where $\underline{g}\ (\underline{g}^T)$ is a column (row) vector whose elements are g_i ; g_i is the coupling constant of the bound state to channel i .

Equation (3.12) can be rewritten in terms of

$$\Delta\ =\ \lim_{s\ \to\ s_B}\ (s\ -\ s_B)\ D^{-1}(s)\ . \tag{3.13a}$$

Then we find that

$$\underline{g}\ =\ -\ (\underline{g}^T\ \underline{g})^{-1}\ N(s_B)\ \Delta\underline{g}\ , \tag{3.13b}$$

so that substituting Eq. (3.13b) into Eq. (3.12) yields a formula for $\delta\ s_B$ of similar form to the first-order mass shift formula derived by Dashen and Frautschi.[2]

We find R' by calculating the residue of $A_1(s)$ at $s\ =\ s_B'$,

$$R'\ =\ \widetilde{D}^{-1}(s_B')\ n(s_B')\ K\ D^{-1}(s_B')\ , \tag{3.14}$$

with

$$K = \lim_{s \to s_B'} (s - s_B') [F(s) - (s - s_B)^{-1} \Gamma]^{-1} \qquad (3.15a)$$

$$= F^{-1}(s_B') \; \Gamma \; F^{-1}(s_B') \; . \qquad (3.15b)$$

The pole-factorization theorem has again been used in obtaining Eq. (3.15b) from Eq. (3.15a). Equation (3.7) relates $F(s)$ to $n(s)$ and $d(s)$.

The factorization theorem satisfied by R' is

$$R_{ij}' = -G_i \; G_j \; . \qquad (3.16)$$

The coupling shift is $\underline{h}$ if $\underline{G} = \underline{g} + \underline{h}$. Setting R' equal to the right side of Eq. (3.14) yields an equation that contains zeroth-order terms. It is difficult to solve for $\underline{h}$ since the equation is not linear. However, a more useful equation for application to a perturbation expansion of the coupling shifts can be obtained by substituting the mass-shift formula into Eqs. (3.14) and (3.15). We also set

$$D^{-1}(s_B') = N^{-1}(s_B') \; R(s_B' - s_B)^{-1} + N^{-1}(s_B') \; \beta(s_B') \; , \qquad (3.17)$$

where $\beta(s)$ is the background term, i.e., it is the unperturbed amplitude minus the pole at s_B . It is of order R . The zeroth-order terms cancel and after some manipulations, we find

$$g_i h_j + h_i g_j + h_i h_j = (X_1 X_2 - X_1 - X_2) g_i g_j + (1 - X_2) g_i b_j$$

$$+ (1 - X_1) b_i' g_j + b_i' b_j , \qquad (3.18a)$$

where

$$X_1 = \underline{g}^T \widetilde{N}^{-1}(s_B) \, n(s_B) \, F^{-1}(s_B') \, [N^{-1}(s_B') - N^{-1}(s_B)] \, (s_B' - s_B)^{-1} \, \underline{g} ,$$

$$(3.18b)$$

$$X_2 = \underline{g}^T [\widetilde{N}^{-1}(s_B') \, n(s_B') - \widehat{N}^{-1}(s_B) \, n(s_B)] \, (s_B' - s_B)^{-1}$$

$$\times F^{-1}(s_B') \, N^{-1}(s_B) \, \underline{g} , \qquad (3.18c)$$

$$\underline{b}^T = \underline{g}^T \widetilde{N}^{-1}(s_B) \, n(s_B) \, F^{-1}(s_B') \, N^{-1}(s_B') \, \beta(s_B') , \qquad (3.18d)$$

$$\underline{b}' = \widetilde{\beta}(s_B') \, \widetilde{N}^{-1}(s_B') \, n(s_B') \, F^{-1}(s_B') \, N^{-1}(s_B) \, \underline{g} . \qquad (3.18e)$$

The leading terms of X_1, X_2, $\underline{b}$, and $\underline{b}'$ are first order in the perturbations.

Equations (3.12) and (3.18) are the exact mass- and coupling-shift formulas when the pole position does not change sheets under the influence of the perturbation.

IV. PERTURBATION THEORY

Equations (3.12) and (3.18), along with the equations of Section II, are sufficient to generate a perturbation expansion for the mass and coupling shifts. The zeroth-order iteration of the perturbed amplitude equations leads to results which are identical to the first order Dashen-Frautschi formulas.[2] The first order iteration of the perturbed amplitude equations is used in the second-order mass and coupling shifts. We only display the second-order mass-shift formula since it is straightforward to derive other terms in the expansion. The higher-order terms in the expansions are probably of little use in numerical calculations.

The application of the reduction procedure of Section II to Eq. (3.3) yields a set of non-Cauchy-singular equations that are identical to Eqs. (2.16) through (2.19), except that the term,

$$- [m^{(-)} (s_B)]^{-1} \Gamma (s - s_B)^{-1} , \tag{4.1a}$$

must be added to the right side of Eq. (2.18a), and the term,

$$- \frac{1}{\pi} \int_R ds' \frac{\tau(s') [m^{(-)}(s_B)]^{-1} \Gamma}{(s' - s + i\epsilon) (s' - s_B)} , \tag{4.1b}$$

must be added to the right side of Eq. (2.19a) .

To generate a perturbation series for δs_B , we need the first several iterations of Eq. (2.18a) and (2.19b) ,

$$f(s) = I + f^{(1)}(s) + \cdots \tag{4.2a}$$

$$u(s) = w(s) + u^{(2)}(s) + \cdots \tag{4.2b}$$

where $f^{(j)}(s)$ and $u^{(j)}(s)$ are of j-the order in the perturbations $\delta\rho$ and V', and $u^{(1)}(s)$ is denoted by $w(s)$.

1. First-Order Mass Shift.

Since Eq. (2.19) is already first order in the perturbation, the first-order mass shift is simply

$$\delta\ s_B\ =\ -\underline{g}^T\ \widetilde{N}^{-1}(s_B)\ w(s_B)\ N^{-1}(s_B)\ \underline{g}\ , \tag{4.3}$$

where

$$w(s)\ =\ \frac{1}{\pi}\int_L ds'\ \frac{\widetilde{D}(s')\ V'(s')\ D(s')}{s'\ -\ s\ +\ i\epsilon}$$

$$+\ \frac{1}{\pi}\int_R ds'\ \frac{\widetilde{N}(s')\ \delta\rho(s')\ N(s')}{s'\ -\ s\ -\ i\epsilon}\ . \tag{4.4}$$

The Dashen-Frautschi result[2] is recovered by inserting Eq. (3.13b) for g and g^T .

2. First-Order Coupling Shift.

As in Reference 2, we define

$$\Delta'\ =\ \frac{d}{ds}\ N^{-1}(s_B)\ R\ +\ N^{-1}(s_B)\ \beta(s_B) \tag{4.5a}$$

$$=\ \frac{d}{ds}\ [(s\ -\ s_B)\ D^{-1}(s)]_{s=s_B}\ . \tag{4.5b}$$

The first order, Eq. (3.18) becomes

$$g_i h_j\ +\ g_j h_i\ =\ -\ (\widetilde{\Delta}'\ w(s_B)\ \Delta\ +\ \widetilde{\Delta}\ w'(s_B)\ \Delta\ +\ \widetilde{\Delta}\ w(s_B)\ \Delta')_{ij}\ . \tag{4.6}$$

The first-order Dashen-Frautschi result follows from Eq. (4.6) as shown in footnote 8 of Ref. 2,

$$\underline{h} = -(\underline{g}^T \underline{g})^{-1} (\tilde{\Delta}' w(s_B) \Delta + \frac{1}{2} \tilde{\Delta} w'(s_B) \Delta) \underline{g} . \tag{4.7}$$

3. Second-Order Mass Shift.

The second-order mass shift is

$$\delta_{(2)} s_B = \underline{g}^T \tilde{N}^{-1}(s_B) \left\{ \frac{1}{\pi} \int_L ds' L(s') \left[\frac{U(s') - U(s_B)}{s' - s_B} \right. \right.$$

$$\left. + \frac{\Gamma^{(1)}}{(s' - s_B - i\epsilon)(s' - s_B)} \right] + \frac{1}{\pi} \int_R ds' T(s')$$

$$\times \left[\frac{U(s') - U(s_B)}{s' - s_B} + \frac{\Gamma^{(1)}}{(s' - s_B - i\epsilon)(s' - s_B)} \right]$$

$$\left. - \frac{1}{\pi} \int_R ds' \frac{\tilde{N}(s') \delta\rho(s') \tilde{D}^{-1}(s') w(s')}{s' - s_B - i\epsilon} \right\} N^{-1}(s_B) \underline{g} \tag{4.8}$$

where

$$U(s) = \frac{1}{\pi} \int_R \frac{ds' \tilde{D}^{-1\dagger}(s')}{s' - s - i\epsilon} [\rho(s') \tilde{D}^{-1}(s') w(s') + \delta\rho(s') N(s')] , \tag{4.9a}$$

$$\Gamma^{(1)} = N^{-1}(s_B) R \tilde{N}^{-1}(s_B) w(s_B) , \tag{4.9b}$$

$$L(s) = \tilde{D}(s) V'(s) D(s) , \tag{4.9c}$$

$$T(s) = \tilde{N}(s) \delta\rho(s) N(s) . \tag{4.9d}$$

Equation (4.8) is the second-order mass shift for both stable particles and resonances. In the case of a resonance shift, R is a set of contours that goes below s_B .

ACKNOWLEDGMENT